

# **Assessment of Patellar Laxity in the *in vitro* Native Knee**

By

**Mark C. Komosa**

Submitted to the graduate degree program in Bioengineering and the Graduate Faculty of the University of Kansas in partial fulfillment of the requirements for the degree of Master of Science.

---

Dr. Lorin Maletsky, Chairperson

---

Dr. Kenneth Fischer, Committee Member

---

Dr. Janice Loudon, Committee Member

Date Defended: December 19<sup>th</sup>, 2011

The Thesis Committee for Mark C. Komosa  
certifies that this is the approved version of the following thesis:

**Assessment of Patellar Laxity in the *in vitro* Native Knee**

---

Dr. Lorin Maletsky, Chairperson

---

Dr. Kenneth Fischer, Committee Member

---

Dr. Janice Loudon, Committee Member

Date Defended: December 19<sup>th</sup>, 2011

## **Abstract**

Patellofemoral joint laxity is a multifactor problem that depends on the active stabilization from the quadriceps muscles, the passive stabilization from the ligaments and retinacular tissue in the PF joint, and the static stabilization from the articular geometries of the distal femur and patella. A custom patellar laxity instrument was designed and built to measure *in vitro* patellar laxity. The instrument measured patellar laxity envelopes through the knee flexion range for ten cadaveric knees by applying a displacement force to the patella and measuring the resultant displacement of the patella. Distinct load levels were found through the flexion range. The largest amount of patellar laxity occurred in early knee flexion ( $\leq 20^\circ$ ) and laxity decreased with flexion after  $20^\circ$  knee flexion. The epicondylar width, sulcus angle, lateral trochlear slope, and medial trochlear slope were measured from MR images of the knees to correlate changes in patellar laxity variation with femoral articular geometry. Principal Component models for shift and tilt laxity were developed to assess the variation in patellar laxity. Over 78% of the variation in shift and tilt laxity was explained by the first three Principal Components. The dominant mode of variation for shift and tilt were the overall amount of laxity through the flexion range is attributed to epicondylar width and sulcus angle. Patellar shift ROM was larger through knee flexion when the subjects had smaller epicondylar width and larger sulcus angle. Another cause of variation was medial and stiffness of the PF joint which was correlated to medial trochlear slope. Subjects with more medial stiffness than the mean also had a steeper medial trochlear fact. Variation in the stiffness of the lateral retinaculum may also be contributing to the variation in medial PF joint stiffness.

## **Acknowledgements**

This thesis is the result of a collaborative effort from several people, and I owe a special thanks to them.

- To my beautiful wife, Sarah, for all your love and unbelievable amount of patience, support, and encouragement you always have as we take on our adventures together. This thesis is as much your accomplishment as it is mine.
- To my advisor, Dr. Lorin Maletsky for always challenging me and for investing so much of his time and energy into teaching and developing me and my fellow students.
- To Dr. Ken Fischer, Dr. Janice Loudon, and the other faculty members at the School of Engineering and KU Medical Center for always teaching and guiding.
- To my fellow graduate students in the lab, Adam, Kaity, Sami, Amit, and Amber for spending many, many long hours and nights working in the lab and for always lending a brain and a helping hand.
- To DePuy Orthopaedics, a Johnson & Johnson company, for funding this research.

## Table of Contents

Abstract.....	iii
Acknowledgements.....	iv
List of Abbreviations .....	vi
List of Figures.....	vii
List of Tables .....	xi
Chapter 1: Introduction.....	1
Chapter 2: Literature Review.....	3
2.1 Patellofemoral Instability.....	3
2.2 Active Stabilizers: Musculature.....	4
2.3 Passive Stabilizers: PF Retinaculum and Ligaments.....	6
2.4 Static Stabilizer: Articular Surfaces.....	8
2.5 Total Knee Arthroplasty .....	10
2.6 Current Methods in Patellar Laxity Assessment.....	12
2.6.1 Imaging Assessment of Patellar Instability.....	12
2.6.2 Clinical Assessments of Patellar Stability.....	14
2.6.3 Current Methods in Measurement of Patellar Laxity.....	15
2.7 Figures .....	18
Chapter 3: Assessment of <i>in vitro</i> Patellar Laxity of the Native Knee.....	23
3.1 Introduction.....	23
3.2 Methods .....	25
3.2.1 Knee Preparation.....	25
3.2.2 Femoral Shape Measurements.....	25
3.2.3 Laxity Assessments.....	26
3.2.4 Knee Kinematic Coordinate Systems.....	27
3.2.5 Calculating PF Joint Laxity.....	27
3.2.6 Principal Component Analysis.....	28
3.2.7 Intra-user Variability.....	29
3.3 Results.....	30
3.3.1 Patellar Laxity Envelopes.....	30
3.3.2 Femoral Shape Measures.....	31
3.3.3 Principal Component Analysis.....	31
3.3.4 Intra-user Variability.....	32
3.4 Discussion.....	33
3.5 Tables and Figures.....	38
Chapter 4: Conclusions.....	51
Chapter 5: References.....	54
Appendix A: Additional Table and Figures.....	63

## **List of Abbreviations**

ANOVA	Analysis of Variance
AP	Anterior-Posterior
BMI	Body Mass Index
IREL	Infrared Emitting Diodes
ITB	Iliotibial Band
EW	Epicondylar Width
LTS	Lateral Trochlear Slope
MTS	Medial Trochlear Slope
ML	Medial-Lateral
MPFL	Medial Patellofemoral Ligament
MR	Magnetic Resonance
PC	Principal Components
PF	Patellofemoral
PLI	Patellar Laxity Instrument
ROM	Range of Motion
SA	Sulcus Angle
SD	Standard Deviation
SI	Superior-Inferior
TKA	Total Knee Arthroplasty
VMO	Vastus Medialis Obliquus
VLO	Vastus Lateralis Obliquus

## List of Figures

- Figure 2-1: The orientations of the individual heads of the quadriceps in the coronal plane (A) and the sagittal plane (B) (Reproduced, with permission, from: Amis, A.A., Current concepts on anatomy and biomechanics of patellar stability. Sports Med Arthrosc, 2007). ..... 18
- Figure 2-2: Weight-bearing AP radiograph assesses overall varus/valgus alignment of knee and joint space narrowing in the knee. (Reproduced, with permission, from: Allen, J.E. and K.S. Taylor, Physical examination of the knee. Prim Care, 2004. 31(4): p. 887-907.) ..... 19
- Figure 2-3: A lateral view radiograph evaluates patellar alta/baja. (Reproduced, with permission, from: Allen, J.E. and K.S. Taylor, Physical examination of the knee. Prim Care, 2004. 31(4): p. 887-907.)..... 19
- Figure 2-4: A true lateral radiograph can identify trochlear dysplasia, as seen by the crossing sign, hypoplastic medial condyle (double contour), and trochlear spur. (Reproduced, with permission, from: Dejour, D. and B. Le Coultre, Osteotomies in patello-femoral instabilities. Sports Med Arthrosc, 2007. 15(1): p. 39-46.) ..... 20
- Figure 2-5: Merchant view x-ray. (Reproduced, with permission, from: Allen, J.E. and K.S. Taylor, Physical examination of the knee. Prim Care, 2004. 31(4): p. 887-907.).... 20
- Figure 2-6: The sulcus angle angle  $BAC$  is measured from the highest point of the medial (B) and lateral (C) facets and the lowest point in the trochlear groove (A) in the Merchant radiograph. The sulcus angle is bisected by  $AO$ , and line  $AD$  passes through the lowest point on the articular ridge of the patella. The congruence angle is angle  $DAO$ . If  $AO$  is medial to  $AD$ , the congruence angle is a negative value, and if  $AO$  is lateral to  $AD$  it is a positive value(Reproduced, with permission, from: Moon, Y.W., et al., Variability in femoral component rotation reference axes measured during navigation-assisted total knee arthroplasty using gap technique. J Arthroplasty, 2010. 25(2): p. 238-43.)..... 21
- Figure 2-7: The patellar tilt angle is measured with a line passing through the medial and lateral edges of the patella and a horizontal line. (Reproduced, with permission, from: Benjamin, J. and M. Chilvers, Correcting lateral patellar tilt at the time of total knee arthroplasty can result in overuse of lateral release. J Arthroplasty, 2006. 21(6 Suppl 2): p. 121-6.)..... 21
- Figure 2-8: The patellar mobility test examines ML patellar stability. The PF joint is divided into four quadrants and patellar laxity is determined by the total translation of the patella when the clinician pushes the patella medially and laterally. (Reproduced, with permission, from: Arendt, E.A., D.C. Fithian, and E. Cohen, Current concepts of lateral patella dislocation. Clin Sports Med, 2002. 21(3): p. 499-519.) ..... 22
- Figure 3-1: Femoral shape measurements quantified from axial MR image. The femoral epicondylar width (EW) is the distance from the medial epicondyle to the lateral

epicondyle. The medial and lateral trochlear are defined as the lines from the deepest point in the trochlear sulcus to the most anterior point of the medial and lateral bony landmarks of the trochlear groove. The sulcus angle (SA) is the angle between the medial and lateral trochlear facets. The medial trochlear slope (MTS) is the angle defined by the medial facet and the posterior condylar axis, the axis tangent to the posterior condyles (dash line). The lateral trochlear slope (LTS) is the angle between lateral facet and the posterior condylar axis..... 41

Figure 3-2: The experimental setup of patellar laxity envelope assessment performed on the *in vitro* specimens. PF and TF kinematics were recorded through the motion tracking arrays of infrared emitting diodes attached to the femur, tibia, and patella..... 42

Figure 3-3: (A) The custom PF laxity instrument (PLI) used to apply an external load on the patella at various flexion angles. (B) Loads to the patella are measured with an in-line axial load cell contained within the laxity instrument, and the direction of the load is captured through the motion tracking array mounted on the instrument. (C) The kinematic response of the patella to the applied load is measured with the motion tracking array attached to the patella. .... 43

Figure 3-4: Local bone coordinate systems were created on the femur, tibia, and patella (red arrows) using bony anatomical features on each bone (yellow stars). The most posterior points on the medial and lateral femoral condyles, the most distal point between the condyles, and the center of the femoral head were used on the femur. The centers of the medial and lateral tibial plateaus, the most proximal points between the tibial eminences, and the center of the intermedullary canal in the distal tibia. .... 44

Figure 3-5: (A) The three-cylindrical open chain system (red lines) used to calculate patellar rotations. The ML link was fixed to the femur, the SI axis was fixed to the patellar, and the AP axis was the cross product the ML and SI axes. Patellar tilt (red arrow) is rotation of the patella about the SI axis with the lateral side of the patella moving posteriorly defined as lateral (+) tilt. (B) Patellar translations are described as translation of the patellar origin relative to the femoral origin (yellow stars) along the fixed femoral coordinate system (green arrows). .... 45

Figure 3-6: Raw experimental patellar shift data (A) and patellar tilt data (B) (yellow) collected during PF envelope assessment for a specific specimen. Data points were extracted at different load levels (-30 N to 30 N) through the flexion range from the PFI load cell (colored points) , and fourth-order polynomials were fit to the extracted data points (solid lines (lateral loads) and dash lines (medial loads)). .... 46

Figure 3-7: Patellar shift (A) and patellar tilt (B) displacements were calculated from the polynomials at each load level through the flexion range for the same specimen in Fig. 3-6). .... 46

Figure 3-8: (A) Mean patellar shift and (B) patellar tilt laxity envelopes. The shaded areas represent  $\pm 1$  standard deviation for their respective load level. No significant differences between medial and lateral patellar excursions for the 10 N load were found in shift or

tilt. Flexion angles where the medial excursions differed significantly from the lateral excursions from a 20 N load (◆) and 30 N load (★) are indicated . All three load levels were significantly different from each other in medial and lateral patellar shift for all flexion angles. The load levels were distinct from each other in lateral tilt from 0° to 80°. The 10 N, 20 N, and 30 N loads were significantly different in medial tilt between full extension and 40° knee flexion. .... 47

Figure 3-9: (A) Mean patellar shift ROM and (B) mean tilt ROM under each load level with the shaded areas as ± 1 standard deviation. Significant differences were found between each of the load levels in shift ROM for all flexion angles and in tilt ROM from 0° to 80° flexion. .... 48

Figure 3-10: PCA perturbation results for patellar shift laxity. The mean excursions (middle column) under ±10 N (blue), ±20 N (green), and ±30 N (red) (positive loads (solid lines) and negative loads (dashed lines)) were perturbed by ±2 standard deviations (-2SD (left column) and +2SD (right column)) along each principal component. The first three PCs explained 86.2% of the variance in the patellar shift laxity data for the ten knees. .... 49

Figure 3-11: PCA perturbation results for patellar tilt laxity. The mean excursions (middle column) under ±10 N (blue), ±20 N (green), and ±30 N (red) (positive loads (solid lines) and negative loads (dashed lines)) were perturbed by ±2 standard deviations (-2SD (left column) and +2SD (right column)) along each principal component. The first three PCs explained 80.4% of the variance in the patellar shift laxity data for the ten knees. .... 50

Figure A-1: Experimental patellar shift data (A) and patellar tilt data (B) collected during PF envelope assessment for a Knee 1. Data points were extracted at each load level, and fourth-order polynomials were fit to the extracted data points (solid lines (lateral loads) and dash lines (medial loads). Patellar shift (C) and patellar tilt (D) displacements were calculated from the polynomials at each load level through the flexion range. .... 65

Figure A-2: Experimental patellar shift data (A) and patellar tilt data (B) collected during PF envelope assessment for a Knee 2. Data points were extracted at each load level, and fourth-order polynomials were fit to the extracted data points (solid lines (lateral loads) and dash lines (medial loads). Patellar shift (C) and patellar tilt (D) displacements were calculated from the polynomials at each load level through the flexion range. .... 66

Figure A-3: Experimental patellar shift data (A) and patellar tilt data (B) collected during PF envelope assessment for a Knee 3. Data points were extracted at each load level, and fourth-order polynomials were fit to the extracted data points (solid lines (lateral loads) and dash lines (medial loads). Patellar shift (C) and patellar tilt (D) displacements were calculated from the polynomials at each load level through the flexion range. .... 67

Figure A-4: Experimental patellar shift data (A) and patellar tilt data (B) collected during PF envelope assessment for a Knee 4. Data points were extracted at each load level, and fourth-order polynomials were fit to the extracted data points (solid lines (lateral loads)

and dash lines (medial loads). Patellar shift (C) and patellar tilt (D) displacements were calculated from the polynomials at each load level through the flexion range. .... 68

Figure A-5: Experimental patellar shift data (A) and patellar tilt data (B) collected during PF envelope assessment for a Knee 5. Data points were extracted at each load level, and fourth-order polynomials were fit to the extracted data points (solid lines (lateral loads) and dash lines (medial loads). Patellar shift (C) and patellar tilt (D) displacements were calculated from the polynomials at each load level through the flexion range. .... 69

Figure A-6: Experimental patellar shift data (A) and patellar tilt data (B) collected during PF envelope assessment for a Knee 6. Data points were extracted at each load level, and fourth-order polynomials were fit to the extracted data points (solid lines (lateral loads) and dash lines (medial loads). Patellar shift (C) and patellar tilt (D) displacements were calculated from the polynomials at each load level through the flexion range. .... 70

Figure A-7: Experimental patellar shift data (A) and patellar tilt data (B) collected during PF envelope assessment for a Knee 7. Data points were extracted at each load level, and fourth-order polynomials were fit to the extracted data points (solid lines (lateral loads) and dash lines (medial loads). Patellar shift (C) and patellar tilt (D) displacements were calculated from the polynomials at each load level through the flexion range. .... 71

Figure A-8: Experimental patellar shift data (A) and patellar tilt data (B) collected during PF envelope assessment for a Knee 8. Data points were extracted at each load level, and fourth-order polynomials were fit to the extracted data points (solid lines (lateral loads) and dash lines (medial loads). Patellar shift (C) and patellar tilt (D) displacements were calculated from the polynomials at each load level through the flexion range. .... 72

Figure A-9: Experimental patellar shift data (A) and patellar tilt data (B) collected during PF envelope assessment for a Knee 9. Data points were extracted at each load level, and fourth-order polynomials were fit to the extracted data points (solid lines (lateral loads) and dash lines (medial loads). Patellar shift (C) and patellar tilt (D) displacements were calculated from the polynomials at each load level through the flexion range. .... 73

Figure A-10: Experimental patellar shift data (A) and patellar tilt data (B) collected during PF envelope assessment for a Knee 10. Data points were extracted at each load level, and fourth-order polynomials were fit to the extracted data points (solid lines (lateral loads) and dash lines (medial loads). Patellar shift (C) and patellar tilt (D) displacements were calculated from the polynomials at each load level through the flexion range. .... 74

## List of Tables

Table 3-1: Maximum medial and lateral excursions and ROM for shift and tilt for 10 N, 20 N, and 30 N load levels.....	38
Table 3-2: Mean femoral shape measures for the ten knees that were included in the PC model.....	38
Table 3-3: PC perturbation results for the femoral anatomical measures in the patellar shift PC model. The mean measures were perturbed by $\pm 2$ standard deviations along each principal component. The first three PCs explained 83.2% of the variance in the patellar shift laxity data for the ten knees. ....	39
Table 3-4: PC perturbation results for the femoral anatomical measures in the patellar tilt PC model. The mean measures were perturbed by $\pm 2$ standard deviations along each principal component. The first three PCs explained 78.1% of the variance in the patellar tilt laxity data for the ten knees. ....	39
Table 3-5: PC Interpretations for patellar shift laxity PC model and tilt laxity PC model. ....	40
Table 3-6: The mean range of patellar shift excursion and tilt rotational excursion measures across all flexion angles at 10 N, 20 N, and 30 N load calculated from a single user performing a laxity assessment three times on the same specimen. ....	40
Table A-1: Femoral shape measures quantified in the axial MR image sets for each knee specimen. ....	64

## **Chapter 1: Introduction**

Patellofemoral (PF) instability is one of the most common knee problems that cause people to seek medical attention. A patellar dislocation or subluxation episode can cause chronic knee pain and instability that can be disabling for the patient, especially in young athletes. Patellar instability has an incidence of 5.8 per 100,000 and increases to 29 per 100,000 in adolescent age groups [1, 2]. Over 100 different procedures have been used to treat or prevent patellar instability after the initial injury, but they have not been consistently successful.

Total knee arthroplasty (TKA) is the standard operative treatment to treat osteoarthritis of the knee and has shown improved knee function postoperatively [3]. Patellar instability is not a cause for a patient to receive a primary TKA, but the change in patellar laxity may lead to postoperative complications. The rate of complications after TKA has declined, but revision surgery is still needed after 3-4% of TKA cases [3-5]. The main cause for revision surgery is anterior knee pain which is indicative of PF complications [6-9]. PF complications include patellar instability, patellar component wear, loosening, or failure, and patella fracture [10-12]. The active, passive, and static stabilizers are altered during TKA and results in a postoperative change in patellar laxity. Surgical technique, component positioning and limb alignment, balance of quadriceps extensor mechanism, component design, patellar preparation, and soft-tissue balancing are all factors that can cause change in the stabilizers of the PF joint. A clinician uses a physical examination to assess laxity by moving the patella with their hands and estimating patellar laxity visually and by observing any signs of apprehension by the

patient during the test. The clinical assessments rely on the clinician's experience and the patient's pain tolerance to determine if the patella is stable or unstable. These stability tests do not provide objective measures of patellar laxity. Subject-to-subject variability in patellar laxity makes diagnosing and tracking patellar instability a difficult task. A repeatable, accurate method to measure patellar laxity is needed to properly assess variation in patellar laxity and to track the progress of a treatment option or physical therapy.

The objective of this research is to design and develop a novel technique to measure patellar laxity in the *in vitro* knee and to identify the types of variation in patellar laxity from subject-to-subject through the knee flexion range. The methods used in this research will be used in future research of the Experimental Joint Biomechanics Research Laboratory to measure patellar laxity with simulated pathologies that contribute to patellar laxity and to measure patellar laxity after TKA. The patellar laxity instrument and methods developed in this research will also be used to determine how patellar laxity changes after total knee arthroplasty and how different component designs contribute to patellar laxity after TKA.

The following three chapters detail the steps taken during this research. Chapter 2 is a literature review that includes the different factors that play a role in patellar stability, clinical assessments used to diagnose patellar instability, and experimental methods that seek to measure patellar laxity. Chapter 3 details the experimental method developed to measure patellar laxity with a novel instrument and to identify the modes of variation in patellar laxity. Chapter 4 is an overall summary and evaluation of the experimental methods used in this research and how they can be adapted and used for future work.

## **Chapter 2: Literature Review**

This literature review is focused on understanding patellar laxity and current methods used to observe, measure, and understand the different contributions to patellar laxity. The review covers the different factors that contribute to patellar laxity and how the laxity is clinically assessed in patients who have experienced recurrent instability. A variety of studies have shown different methods to measure indicators that correlate to stability; however, the ability to directly identify the cause of patellar instability is still difficult. Directly measuring patellar laxity to assess stability has more recently been used to understand what can cause instability, but previous studies still have not measured patellar laxity in a clinically feasible manner that can track a patient's progress through treatment or physical therapy.

### **2.1 Patellofemoral Instability**

Patellar instability is defined by symptomatic subluxation or dislocation of the patella from the trochlea of the femur [13]. Patellar instability is a frequent knee problem and relates to anterior knee pain with an incidence of primary patellar dislocation at 5.8 per 100,000 and adolescent age groups experience a higher incidence of 29 per 100,000 [1, 14-17]. Many patients continue to have pain, instability, and limitations in strenuous activities following a primary dislocation with a reported recurrence of 15% to 50% in patients following nonsurgical treatment, and 49% of patients with three or more instability incidents [1, 18, 19]. An instability event, subluxation or dislocation, occurs during a combination knee movement during a traumatic weight bearing or twisting event involving knee flexion followed by acute pain [13, 20]. Patients with recurrent instability generally feel pain where the medial patellofemoral ligament (MPFL) attaches to the

femoral medial epicondyle and express apprehension to patellar mobility tests. A single dislocation or subluxation event can lead to recurrent patellar pain and instability [1, 2, 18, 19, 21-23].

PF joint laxity depends on the interaction of active stabilization from the quadriceps muscles, the passive stabilization from the ligaments and retinacular tissue in the PF joint, and the static stabilization from the articular geometries of the distal femur and patella [17, 24, 25]. In a healthy knee with a stable PF joint, these stabilizers remain balanced during gait, running, jumping, and other activities of knee motion [26].

## **2.2 Active Stabilizers: Musculature**

The quadriceps muscle group is the primary active stabilizer of the PF joint. The quadriceps is made of six discrete muscle heads that insert into the patella and generates forces directly on the patella [27]. The individual muscles insert onto the patella across the entire width of the proximal, medial, and lateral aspects of the patella (Fig. 2-1) [24]. The rectus femoris originates on the anterior surface of the femur, runs parallel along the femur shaft, and inserts directly on the superior pole of the patella. The vastus intermedius parallels and lays deep to the rectus femoris. The vastus medialis and the vastus lateralis originate alongside the proximal femur and converge to the patella in an orientation that diverts from the anatomical axis of the femur with orientations of  $15^\circ$  and  $14^\circ$  from the femur anatomical axis, respectively, in the coronal plane [28, 29]. The vastus medialis and lateralis both have distal portions that deviate a large amount from the femur anatomical axis that have the potential to pull the patella in a medial or lateral direction. The vastus medialis obliquus (VMO) is oriented  $47^\circ \pm 5^\circ$  from the femoral anatomical axis in the coronal plane and pulls the patella medially and posteriorly [26,

28, 30]. The VLO has an orientation of  $35^{\circ} \pm 4^{\circ}$  from the anatomical axis and pulls the patella laterally [24].

The patella is stabilized by the balance between the medial and lateral quadriceps muscles. The sum of the individual quadriceps forces vectors the coronal plane produces a resultant vector that is parallel to the femur bone with a patella that is stable [31]. The VMO and VLO are the primary active medial and lateral stabilizers of the patella [30], and an imbalance in the strength between the VMO and VLO will cause the resultant quadriceps force vector to deviate from the femoral anatomical axis in the coronal plane and may lead to patellar instability. The VMO and VLO muscles also are not parallel to the femoral shaft in the sagittal plane and generate posterior forces on the patella as the muscles contract. The VMO and VLO pull the patella posteriorly when the knee is near full extension, creating a compressive load to seat the patella in the trochlear groove [28].

The VMO is the first muscle of the quadriceps to weaken and can be overtaken by the lateral forces acting on the patella from the VLO causing the patella to displace more laterally and lead to medial patellar instability [30, 32, 33]. The VMO can contribute to a total of 10% of total quadriceps tension based on its physiological cross sectional area [28]. Weakening of the VMO can cause the resultant quadriceps force vector to shift laterally up to 6 degrees from in the coronal plane. Senavongse et al. found that completely relaxing the VMO causes an increase in patellar laxity from knee flexion angles of 0 to 90 degrees. The largest change was seen at 20 degrees knee flexion where relaxing the VMO cause patellar laxity to increase by 30% [14, 15]. Goh et al. found that relaxing the VMO caused the patella to displace 4-5 mm more laterally under a given

load and increased the contact force the patella applied to the lateral facet of the trochlear groove [34].

The VMO attaches to the lateral portion of the medial patellofemoral ligament (MPFL), causing tension in the MPFL as the VMO contracts in early knee flexion angles [35]. Therefore the VMO increases its contribution to patellar stability in early knee flexion with its interaction with the MPFL. The VMO is commonly injured during acute patellar dislocation and may lead to continual patellar instability and further dislocation [36]. VMO weakness and injury can be addressed nonoperatively with exercises to promote VMO activity and regain strength. Patellar taping may be used to optimize the location the patella engages in the trochlear groove [37]. Taping the patella improves VMO strength by increasing quadriceps torque to activate the VMO earlier than the VLO [38, 39]. Some physicians treat VMO injury surgically by repairing the VMO attachment to the MPFL and other ligaments of the medial retinaculum to improve patellar stability [40]. Ahmad et al. showed that repairing a torn VMO by attaching it to the MPFL restored the ability of the VMO to apply a medial force to the patella [41].

### **2.3 Passive Stabilizers: PF Retinaculum and Ligaments**

The PF retinaculum and ligaments are the soft tissues of the PF joint and are the primary passive stabilizers of the PF joint. As the knee moves to full extension, the patella is no longer engaged in the trochlear groove, and patellar stability relies heavily on soft tissue constraint. The MPFL is the primary soft tissue restraint to lateral patellar displacement [14, 35, 36, 42-47]. There are three main layers in the retinaculum and the MPFL is located in the second tissue layer deep to the superficial fascia and superficial the joint capsule as continuation of the deep surface of the distal VMO muscle fibers [48,

49]. The MPFL runs from the proximal medial edge of the patella to the groove between the adductor tubercle and medial epicondyle, anterior to the MCL attachment site [25, 43, 44, 49-51]. The patella is disengaged from the trochlear groove in early flexion, and the MPFL directs the patella into the trochlear groove as the knee flexes in early knee flexion. It is under tension from 0° to 30° knee flexion and becomes more relaxed as knee flexion increases. Previous studies have shown that the MPFL contributes to 50% to 60% of the overall lateral patellar stability from full extension to 30° knee flexion [35, 43-45]. The MPFL is almost always injured during patellar dislocation, since dislocations most commonly occur in early knee flexion [52].

Similar to the medial patellar anatomy, the lateral retinaculum of the PF joint has three layers of soft tissue. The superficial layer is the iliotibial band (ITB), the intermediate is the lateral patellofemoral band, also known as the iliopatellar band, and the deep layer is the PF joint capsule. The lateral PF band is a transversely orientated structure that extends from the deep aspect of the ITB that attaches to the lateral edge of the patella [17, 53]. The band does not directly attach to the femur, but is indirectly attached through the ITB [54, 55]. The ITB causes the patella to track more laterally and contributes to medial patellar stability [56-59]. The lateral retinaculum contributes the most to medial patellar stability at knee flexion angles close to full extension (0° to 30°) [60].

Patellar instability from the PF soft tissues can be treated operatively with a lateral retinacular release, medial repair, or an MPFL reconstruction. Lateral retinacular release has not effectively treated patellar instability, since patients have continued to experience instability post-operatively [61]. Lateral release does not effectively position

the patella in a more medial position and often creates medial patellar instability [62, 63]. Treating patellar instability with surgically repairing the medial retinaculum can improve stability [64, 65]. However, the rate of instability occurrence is similar to nonoperative treatments [66, 67]. MPFL reconstruction replaces the damaged ligament with a graft to restore proper function of the MPFL. The procedure is difficult because malpositioning or using an incorrectly sized graft creates improper graft tension. An overtightened graft increased PF joint contact pressure and may lead to PF arthritis, and an undertightened graft can cause frequent patellar instability [68, 69]. Although MPFL reconstruction is difficult and debated, it has shown good results in preventing future instability [70-72].

#### **2.4 Static Stabilizer: Articular Surfaces**

Patellar stability is influenced by the geometries of the femoral trochlear groove and the articulating surface of the patella. The trochlear groove has a shape that complements the articulating patellar surface and provides additional stability to the patella. The height and slope of the lateral trochlear wall provide stability by resisting lateral patella translation as the knee flexes, and the medial wall resists medial translation [73-75]. If there is an imbalance of forces from the quadriceps the patella must still climb the medial and lateral facet slopes in the trochlear groove to dislocate or sublux. The steepness and depth of the trochlear groove do not remain constant through the groove, so the amount of force required to displace the patella up the facets in the groove are not constant through the trochlear groove. The medial and lateral facets of the trochlear groove are the highest proximally on the anterior aspect of the femur and lower as the groove moves distally and posteriorly [17, 76]. Considerable variation in individual trochlear groove length, width, steepness, and geometry exist [25]. The sulcus angle is a

measure of the steepness of the trochlear groove and is measured using an axial radiography or magnetic resonance (MR) imaging and is defined as the angle between the medial and lateral walls of the trochlear groove [13, 77]. The sulcus angle is dependent on the height and slope of the trochlea. A decrease in the height of the medial or lateral wall indicates a shallow trochlear and decreases the sulcus angle. The normal sulcus angle is approximately  $140^\circ$ , and an angle  $>145^\circ$  is considered a shallow sulcus and sign of trochlear dysplasia [78].

The location of the patella in the trochlear groove is dependent on the knee flexion angle. At full extension, the patella is completely disengaged from the trochlear groove, and patellar stability is controlled by the PF retinaculum and quadriceps muscle forces. When the knee begins to flex past full extension, the MPFL guides the patella into the trochlear groove [44]. The distal edge of the patellar articular surface comes into contact with the proximal trochlear surface, and the contact area increases between the patella and femur as the knee continues to flex [79]. The patella becomes fully engaged in the trochlear groove after  $20^\circ$  to  $30^\circ$  knee flexion. After  $30^\circ$  knee flexion, contributions of the soft tissue in the PF joint to patellar stability are minimized, and the depth, slope, and sulcus angle of the trochlea become the most important stabilizer of the patella [80].

Trochlear dysplasia is a shallow, flattened trochlear groove, and is a significant risk factor for patellar instability. It occurs in less than 2% of the population in the United States and is observed in 85% to 96% of patients with recurring patellar instability [81, 82]. The height and slope of the lateral trochlear facet resists lateral patellar translation and provides lateral patellar stability. A flattened lateral trochlea contributes more to lateral patellar instability than damaged medial retinaculum or VMO weakness [14]. It

decreases the stability through the knee flexion range, and increases the stress on the medial retinaculum since it will have a higher contribution to patellar stability [79]. The static stabilization of the trochlear groove geometry provides a more consistent contribution to patellar stability than the dynamic stabilization from the quadriceps [83]. A higher lateral trochlear wall creates a smaller sulcus angle and leads to improved patellar engagement into trochlear groove and decreased rates of patellar instability in early knee flexion. However, the increased stability from a more conformed trochlear geometry may lead to PF arthritis [84].

Patients with trochlear dysplasia and recurrent patellar instability may receive one of two surgical treatments. The first alters the bony geometry of the trochlear groove known as trochleoplasty, and include Albee trochlear osteotomy, sulcus deepening trochleoplasty, and rotational trochleoplasty [82, 85, 86]. These procedures improve patellar tracking and increase patellar stability by directly deepening the sulcus angle [16, 87]. Trochleoplasty is not often performed because the procedure is difficult to perform and predisposes the patient to PF arthritis [88]. The second option is performed on other factors that will compensate for the flattened trochlea, such as patella alta, damaged medial PF soft tissue, or the distance of the tibial tubercle to the trochlear groove. These procedures can provide additional patellar stability to the patient without directly reconstructing the trochlear groove with a trochleoplasty.

## **2.5 Total Knee Arthroplasty**

Total knee arthroplasty (TKA) is the standard operative treatment to treat osteoarthritis of the knee and has shown improved knee function postoperatively [3]. Patellar instability is not a cause for a patient to receive a primary TKA, but the change in

patellar laxity from the surgery may lead to postoperative complications. The rate of complications after TKA has declined, but revision surgery is still needed after 3-4% of TKA cases [3-5]. The main cause for revision surgery is anterior knee pain which is indicative of PF complications [6-9]. PF complications include patellar instability, patellar component wear, loosening, or failure, and patella fracture [10-12]. The active, passive, and static stabilizers are altered during TKA and results in a postoperative change in patellar laxity. Surgical technique, component positioning and limb alignment, balance of quadriceps extensor mechanism, component design, patellar preparation, and soft-tissue balancing are all factors that can cause change in the stabilizers of the PF joint. Malpositioning of the femoral, tibial, or patellar component has been recognized as the most frequent cause of patellar instability and other PF joint problems [6, 89-98].

The surgical incision during TKA to expose the knee joint will influence patellar laxity. The subvastus and medial parapatellar approaches are commonly used to perform TKA and both surgical approaches compromise the extensor mechanism with incisions that damage the medial quadriceps and the medial PF ligaments and retinaculum [99-101].

During TKA, the surgeon has the option to leave the patella unresurfaced during the procedure or to resurface the patella with a polyethylene component. Many studies have shown that contradictory results regarding clinical outcomes between the resurfaced and unresurfaced patella, and the effects of resurfacing the patella during TKA is not entirely understood [10, 102-111].

Patellar component designs will alter postoperative patellar laxity, and are typically a symmetric dome-shape, a medialized dome, or an anatomical shape. The

native patella is not symmetric or dome-shaped with a ridge that is medial of the center of the patella. The symmetric dome component will be medially placed on the patella to position the center of the dome with the center of the patellar ridge, leaving some part of the patellar bone uncovered. The medialized dome component has a medially placed dome-center that allows the patellar bone to be fully covered while the component is placed on the center of the patella bone. The anatomical component has a medially placed ridge that mimics the articular surface of the native patella. The anatomical components have been shown to have decreased damage compared to a symmetrical dome in a retrieval study, but no correlation was found between patellar component design and patellar stability [112].

## **2.6 Current Methods in Patellar Laxity Assessment**

### *2.6.1 Imaging Assessment of Patellar Instability*

Standard radiographs of the PF joint are used to assess patellar instability. The images are a static measure of the bone geometry and include a weight-bearing AP view, lateral view, and Merchant view. The Weight-bearing AP radiograph evaluates varus/valgus alignment of the knee and determines if there is any joint space narrowing in the knee (Fig. 2-2). The lateral view allows the clinician to assess patellar height (Fig. 2-3). Patella alta is a high-riding patella and baja is a low-riding patella. Patella alta has been related to patellar instability because the patella will engage in the trochlear groove at a higher knee flexion angle than a knee with normal patellar height [113-115]. Dejour et al. found that 24% of patients with patellar instability also had patella alta [81]. Trochlear dysplasia can be seen in a true lateral radiograph when the deepest part of the trochlear groove crosses the anterior aspect of the condyles, known as the crossing sign

(Fig. 2-3). A trochlear spur and hypoplastic medial condyle, seen by a double contour in the trochlear groove are also indicators of trochlear dysplasia in a lateral radiograph. The Merchant view radiograph is an axial view of the patella at 30° knee flexion and assesses degeneration of the PF joint, patellar subluxation, trochlear dysplasia, and overall trochlear geometry (Fig. 2-5) [78]. The orientation and position of the patella in the trochlear groove are determined from the Merchant view with the sulcus angle, congruence angle and patellar tilt angle. The sulcus angle measures the angle of the trochlear groove, and patellar instability is correlated to a shallow trochlear with a sulcus angle larger than 145° (Fig. 2-6) [81]. The congruence angle is an indicator of patellar subluxation. The average congruence angle in a healthy PF joint is  $-8^\circ \pm 6^\circ$  (Fig. 2-6) [116]. The patellar tilt angle measures patellar tilt relative to the femur with the knee at 20° flexion (Fig. 2-7) [117]. The tilt angle opens laterally in the healthy knee, and the angle opens medially or is parallel in patients with recurrent subluxation [118].

Radiograph images provide static measures of the PF joint geometry and the position and orientation of the patella in the trochlear groove, but the images only provide signs of patellar instability. Radiographs to examine patellar stability are taken between 20° and 45° knee flexion, but the patella usually becomes unstable between full extension and 20° flexion. Indicators of instability near extension cannot be seen in radiograph studies. Results from radiographs do not have strong correlations to clinical observations of patellar instability, and many times the injured joint cannot be distinguished from the health contralateral joint [119].

MR images are used to assess the soft tissue structures of the PF joint and can identify damage to the structures, particularly the MPFL. MR image studies are 70%

accurate in detecting MPFL injury when evaluating patellar instability [120]. Other indicators of instability found in MR images include bone contusions of the anterior femur, cartilage damage, retinacular injury, and quadriceps injury [121]. The same measurements can be made from MR images as radiographs, and are considered more useful because the images include the cartilage surface in the measurements [76, 77, 122]. MR images and radiographs, only show signs of instability and are used to confirm a clinical diagnosis from a physical evaluation.

### *2.6.2 Clinical Assessments of Patellar Stability*

A physical examination of the PF joint is used to detect and diagnose patellar instability because the instability is recreated in the assessment. Clinicians most commonly perform the patellar mobility test to assess the stability of the PF joint [61]. The knee is held at 20° to 30° of knee flexion with the quadriceps relaxed. The patella is mentally divided into four quadrants, and the clinician manually displaces the patella medially and laterally with their thumb and index finger to determine the amount of laxity in the PF joint (Fig. 2-8). The clinician estimates the overall patellar laxity based on the number of quadrants the patella displaces [123]. The patellar mobility test is a non-functional exam because it is performed while the patient is sitting, but instability events occur during weight bearing activity. The moving patellar apprehension test a modification of the patellar mobility test exam that better replicates an instability incident [20]. The clinician maintains a medial or lateral force on the patella as the knee is flexed and extended, similar to a pivot shift test for the knee and other dynamic tests to examine joint instability [124-126]. The results of the test depend on the patient orally expressing apprehension or activating their quadriceps to stop the test.

Both the patellar mobility test and the moving patellar apprehension test are used to identify patellar instability and to track the progress of treatment for instability. The progress of a patient's patellar stability can be tracked if patellar laxity can be measured throughout the treatment process. The clinical assessments of patellar stability in a physical examination rely on the clinician's experience and the patient's reaction to the tests to determine if the patella is stable or unstable. If the patient has a high tolerance for pain the clinician may not correctly identify patellar instability. These stability tests do not provide objective measures of patellar laxity. Subject-to-subject variability in patellar laxity makes diagnosing and tracking patellar instability a difficult task.

### 2.6.3 Current Methods in Measurement of Patellar Laxity

Patellar laxity can be quantified by measuring the force needed to displace the patella at various knee flexion angles. Previous studies have measured patellar stability or laxity to better understand the contributions of the active, passive, and static stabilizers to patellar laxity [14-16, 28, 43-45, 60, 127, 128]. Conlan et al. found that the MPFL was the primary passive restraint to *in vitro* patellar displacement at full extension by sequentially cutting the medial soft tissue structures [43]. Farahmand et al. measured lateral patellar force-displacement behavior from 0° to 90° knee flexion in an *in vitro* study [127]. They loaded the quadriceps with static loads in proportion to their cross-sectional area and measured the force required to displace the patella at various displacement levels up to 9 mm. They found that a 5 mm lateral patellar translation required a constant applied force from full extension to 60° knee flexion, with a significant increase in the force at 90° flexion. In another study, Farahmand et al. measured the sulcus angle and depth of the trochlear groove where the patella is engaged

with the trochlear groove through the knee flexion range and found the trochlear groove did not deepen as knee flexion increased [28]. These studies suggest the geometry of the trochlear groove has a large contribution to patellar stability in early knee flexion and that the active stabilization from the muscle forces do not increase the constraint provided by the static and passive stabilizers [28, 127]. They established overall trends in patellar laxity and normal limits of patellar motion through the knee flexion range with force-displacement curves; however the patella was fixed to only allow ML translation and prevented patellar tilt and rotation during the test. Patellar displacement is a coupled motion that includes patellar tilt and rotation as the patella translates medially and laterally.

Senavongse et al. established the forces required to displace the patella medially and laterally up to 10mm between 0° and 90° knee flexion [15]. They found that medial and lateral stability are different from one another through the flexion range. The contributions of the active, passive, and static stabilizers to lateral patellar stability were measured by Senavongse and Amis [14]. At full extension the medial retinacular structures had the largest contribution to lateral patellar stability, and its contribution decreased with knee flexion. A relaxed VMO reduced the force needed to displace the patella 10 mm by 30% from 20° to 90° knee flexion. A flattened lateral facet of the trochlear groove had the largest overall effect from 10° to 60° flexion. The trochlear slope had an increasing contribution from 0° to 30° and then steadily decreased through the flexion range. The PF joint became increasingly less stable from full extension to 20° knee flexion, the flexion angle with the greatest amount of patellar instability. After 20° patellar stability increased with flexion angle.

Merican et al. investigated the effects of the lateral retinacular structures on medial patellar stability by selectively cutting the lateral structures [60]. The lateral retinaculum contributes to medial stability through the flexion range but its largest contribution occurred at knee flexion angles of 0° to 30°.

Fithian et al. developed an instrument to measure the displacement of the patella to an applied load of 2.5 lb and 5 lb, similar to instruments used to diagnose cruciate ligament injury in the knee [129-131]. The instrument could not clearly distinguish any difference between a patient's knee with patellar instability and their health contralateral knee. High variation in the laxity measurement did not lead to significant results and did not demonstrate the efficacy of this instrument in measuring patellar laxity or diagnosing instability.

Egusa et al. sought to create objective parameters to clinically diagnose patellar instability by measure force-displacement curves during a clinical assessment [132]. The patellar laxity measurement taken at a 5 mm patellar displacement was correlated to the diagnosis of patellar instability. However, the diagnosis was still based on a subjective evaluation.

Although these studies have been important to better understanding patellar instability and how the different stabilizers can contribute to a patient experiencing instability, there is not a good understanding of how patellar laxity can change and vary from subject-to-subject. Subject-to-subject variability in joint geometry, musculature strength and orientation, and ligament stiffness makes it difficult to measure laxity. There is a need to develop method that can objectively measure patellar laxity, and determine how the change in laxity can be attributed to variation in the active stabilization of the

quadriceps muscles, the passive stabilization of the retinaculum, and the static stabilization of the articular geometry.

## 2.7 Figures

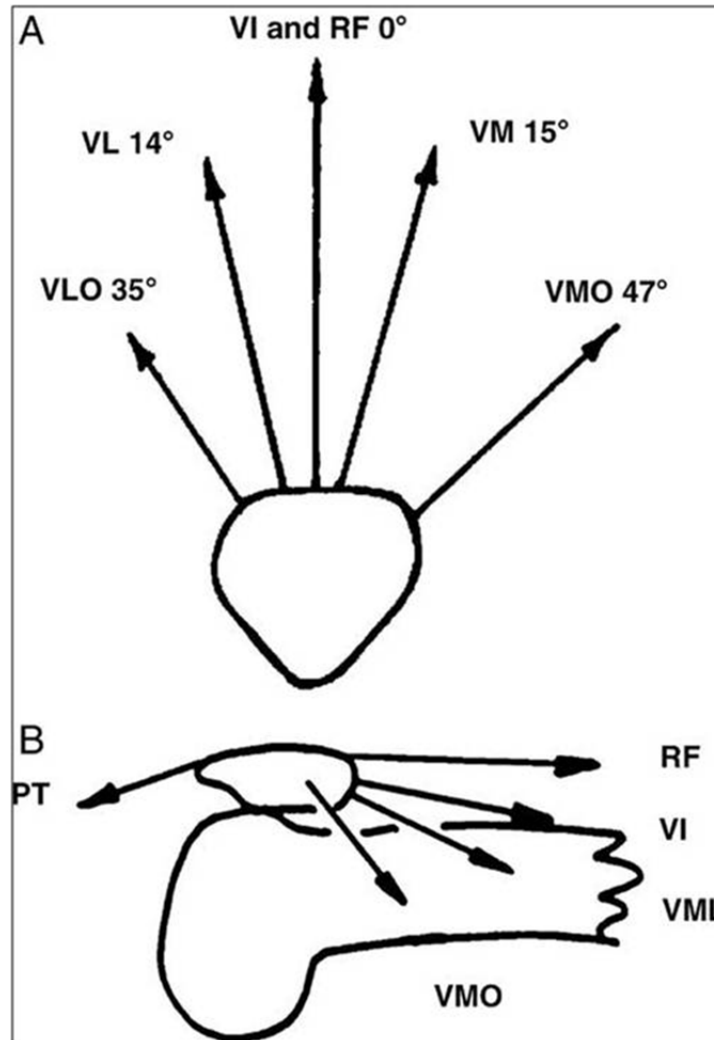


**Figure 2-1: The orientations of the individual heads of the quadriceps in the coronal plane (A) and the sagittal plane (B) (Reproduced, with permission, from: Amis, A.A., Current concepts on anatomy and biomechanics of patellar stability. Sports Med Arthrosc, 2007).**



**Figure 2-2: Weight-bearing AP radiograph assesses overall varus/valgus alignment of knee and joint space narrowing in the knee. (Reproduced, with permission, from: Allen, J.E. and K.S. Taylor, Physical examination of the knee. Prim Care, 2004. 31(4): p. 887-907.)**



**Figure 2-3: A lateral view radiograph evaluates patellar alta/baja. (Reproduced, with permission, from: Allen, J.E. and K.S. Taylor, Physical examination of the knee. Prim Care, 2004. 31(4): p. 887-907.)**

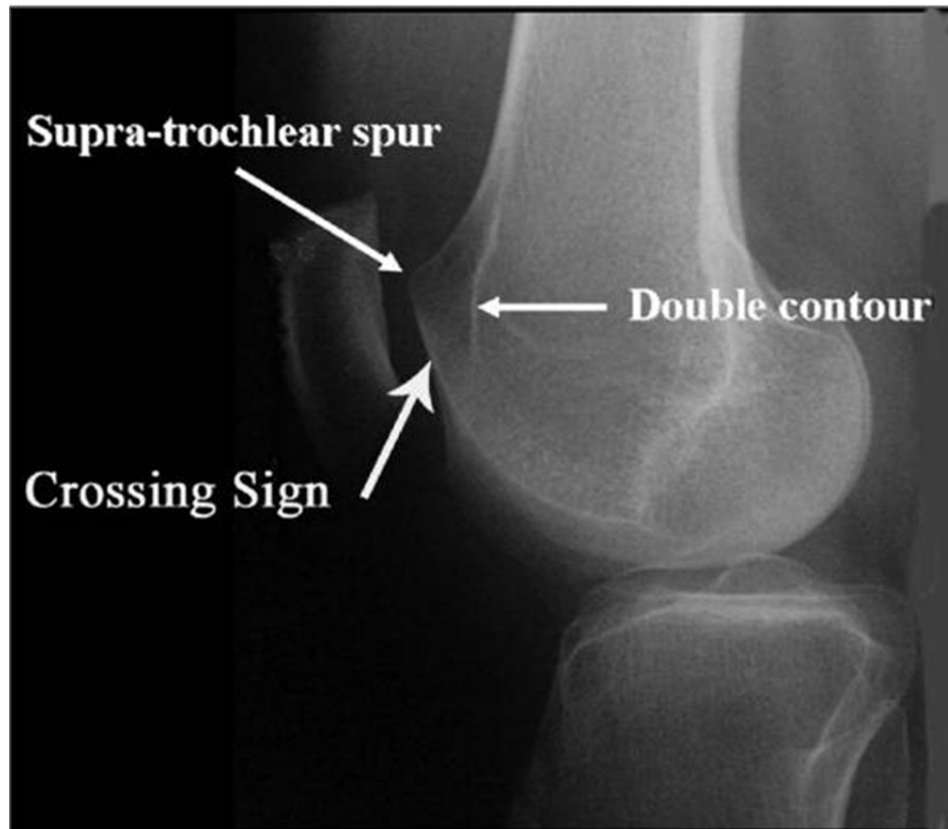


**Figure 2-4: A true lateral radiograph can identify trochlear dysplasia, as seen by the crossing sign, hypoplastic medial condyle (double contour), and trochlear spur. (Reproduced, with permission, from: Dejour, D. and B. Le Coultre, Osteotomies in patello-femoral instabilities. Sports Med Arthrosc, 2007. 15(1): p. 39-46.)**

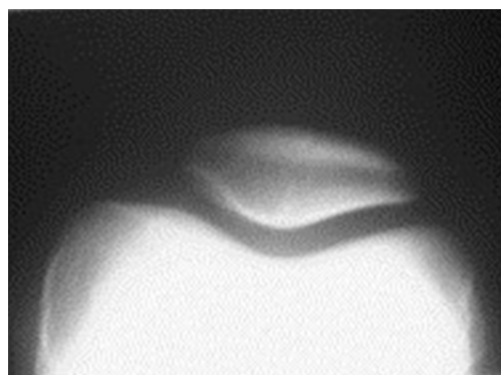


**Figure 2-5: Merchant view x-ray. (Reproduced, with permission, from: Allen, J.E. and K.S. Taylor, Physical examination of the knee. Prim Care, 2004. 31(4): p. 887-907.)**

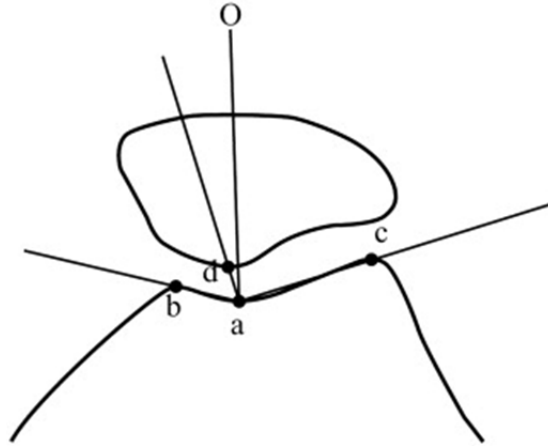


**Figure 2-6: The sulcus angle angle  $BAC$  is measured from the highest point of the medial (B) and lateral (C) facets and the lowest point in the trochlear groove (A) in the Merchant radiograph. The sulcus angle is bisected by  $AO$ , and line  $AD$  passes through the lowest point on the articular ridge of the patella. The congruence angle is angle  $DAO$ . If  $AO$  is medial to  $AD$ , the congruence angle is a negative value, and if  $AO$  is lateral to  $AD$  it is a positive value(Reproduced, with permission, from: Moon, Y.W., et al., Variability in femoral component rotation reference axes measured during navigation-assisted total knee arthroplasty using gap technique. *J Arthroplasty*, 2010. 25(2): p. 238-43.)**

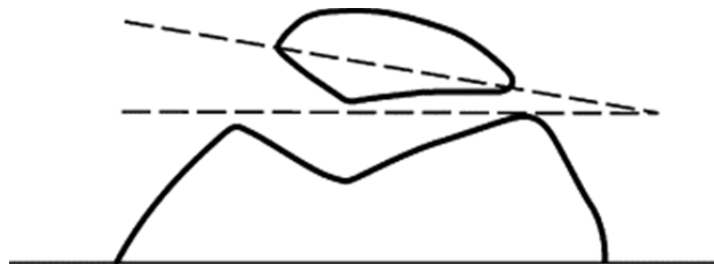


**Figure 2-7: The patellar tilt angle is measured with a line passing through the medial and lateral edges of the patella and a horizontal line. (Reproduced, with permission, from: Benjamin, J. and M. Chilvers, Correcting lateral patellar tilt at the time of total knee arthroplasty can result in overuse of lateral release. *J Arthroplasty*, 2006. 21(6 Suppl 2): p. 121-6.)**

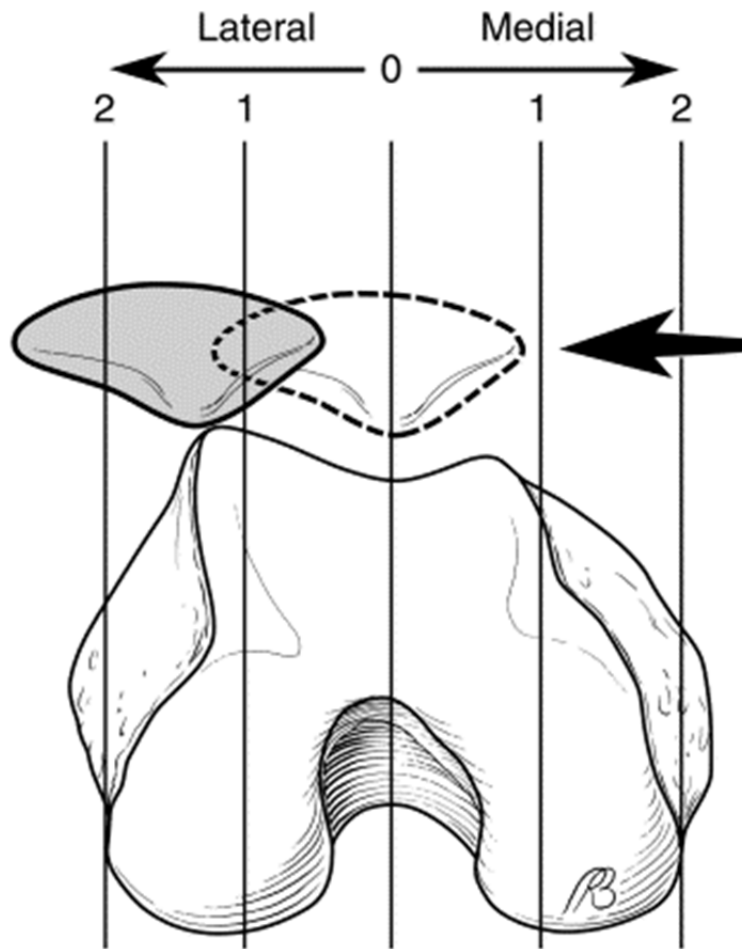


**Figure 2-8: The patellar mobility test examines ML patellar stability. The PF joint is divided into four quadrants and patellar laxity is determined by the total translation of the patella when the clinician pushes the patella medially and laterally. (Reproduced, with permission, from: Arendt, E.A., D.C. Fithian, and E. Cohen, Current concepts of lateral patella dislocation. Clin Sports Med, 2002. 21(3): p. 499-519.)**

## **Chapter 3: Assessment of *in vitro* Patellar Laxity of the Native Knee**

### **3.1 Introduction**

Total knee arthroplasty (TKA) is the standard operative treatment to treat osteoarthritis of the knee and has shown improved knee function postoperatively [3]. Patellar instability is not a cause for a patient to receive a primary TKA, but the change in patellar laxity may lead to postoperative complications. The rate of complications after TKA has declined, but revision surgery is still needed after 3-4% of TKA cases [3-5]. The main cause for revision surgery is anterior knee pain which is indicative of PF complications [6-9]. PF complications include patellar instability, patellar component wear, loosening, or failure, and patella fracture [10-12]. The active, passive, and static stabilizers are altered during TKA and results in a postoperative change in patellar laxity. Surgical technique, component positioning and limb alignment, balance of quadriceps extensor mechanism, component design, patellar preparation, and soft-tissue balancing are all factors that can cause change in the stabilizers of the PF joint. PF joint laxity is a multifactor problem that depends on the active stabilization from the quadriceps muscles, the passive stabilization from the ligaments and retinacular tissue in the PF joint, and the static stabilization from the articular geometries of the distal femur and patella [17]. The contributions from each of these factors remain unclear, and proper treatment of patellar instability requires an understanding of the interactions between these factors.

Patellar instability is typically not observed while the joint is at rest, so clinical diagnosis depends on the patellar displacement response, known as excursion, to the application of a force applied to the patella [61, 128, 133, 134]. The clinician manually displaces the patella with their thumb and index finger to determine the amount of laxity

in the PF joint, and relies on their training and experience to determine if the patella is unstable or stable [20, 61]. Patellar laxity has been previously measured with the application of specific loads on the patella, ranging 11 to 80 N, and many patients experience apprehension at a load application of 11N on the patella [128, 130, 132, 134].

Although these studies have been important to measuring patellar laxity and to understand the contributions of the different stabilizers to patellar laxity, subject-to-subject variability in patellar laxity, joint geometry, musculature strength and orientation, and ligament stiffness makes comparing laxity between subjects a difficult task. The change in patellar laxity after TKA can lead to PF complications and revision surgery, and there is currently not a good understanding of how the change in the active, passive, and static stabilizers change during TKA affect the resulting postoperative patellar laxity. There is a need to develop method that can measure patellar laxity throughout the flexion range and to determine how the change in laxity can be attributed to variation in the active stabilization of the quadriceps muscles, the passive stabilization of the retinaculum, and the static stabilization of the articular geometry. The purpose of this study was to use a patellar laxity instrument to measure *in-vitro* patellar laxity and to identify modes of subject-to-subject variation in patellar laxity. The hypothesis was that primary mode of variation would be overall patellar range of motion (ROM) through the flexion range and this variation would be attributed to overall femur bone size and the sulcus angle.

## 3.2 Methods

### 3.2.1 Knee Preparation

Ten whole cadaveric legs were acquired (age:  $65 \pm 13$  years, BMI:  $23.6 \pm 13.3$ ) for this study. Each leg was screened for prior knee injury or knee surgery and thawed at room temperature for 24 hours prior to test. MR images were acquired for each knee using a 1.5 T Siemens scanner (Siemens Healthcare, Erlangen, Germany). The sequence protocol for each knee was a sagittal isotropic 3D T2-weighted steady-state free-precession (TRUFI) sequence with water excitation (we) and 1 mm slice thickness. The femur was sectioned 225 mm proximal to the epicondylar axis, and the tibia was sectioned 175 mm distal to the epicondylar axis. Soft tissue beyond 130 mm from the epicondylar axis was removed to preserve the knee joint capsule, and the quadriceps musculature was isolated from the surrounding tissue. The femur and tibia were potted in aluminum fixture tubes with bone cement so the bone was concentric with the fixture.

### 3.2.2 Femoral Shape Measurements

Femoral shape measurements that relate to patellar laxity were collected from the MR images for each knee. The sagittal MR image set for each knee was resliced to create an axial image set, and the axial slice containing the widest femoral epicondylar width was identified and femoral shapes measures were calculated. Epicondylar width (EW), sulcus angle (SA), lateral trochlear slope (LTS), and medial trochlear slope (MTS) were quantified in this plane (Fig. 3-1) [76, 77, 116, 122].

### 3.2.3 Laxity Assessments

The proximal femur of each knee was rigidly mounted to the base plate of a muscle loading rig (Fig. 3-2), and the rectus femoris and vastus intermedius tendons were loaded with a total of 22 N along the long axis of the femur. Infrared light emitting diode (IRED) motion tracking arrays were mounted to the femoral and tibial fixtures, and one was directly fastened on the anterior side of the patella.

Each knee was manually flexed from full extension to terminal flexion with a constant 22 N quadriceps load and no external displacement loads applied to the knee. A medial and lateral patellar laxity envelope was performed on each knee with a custom patellar laxity instrument (PLI) comprised of three components: the PLI base, an in-line axial load cell (Omega LC-302-25), and the loading tip (Fig. 3-3A). Loads were applied to the patella during the laxity envelopes by loading the patella with the PLI loading tip which compressed the in-line axial load cell contained in the instrument. The loading tip has enough clearance with the PLI base to allow it to move relative to the base and allowed the user to visually inspect the direction of the applied load. An axial load is applied when the tip remains concentric with the PLI base, and an off-axis load is applied when the tip rocks and is no longer concentric with the PLI base. Load data was captured from the load cell using Labview (National Instruments, Austin, TX), and an IRED motion tracking array was attached to the instrument to measure the orientation of the PLI as the patella was loaded (Fig. 3-3B).

For the medial laxity assessment, the knee was placed at full extension manually and a 30 N medial displacement load was applied to the patella with the PLI (Fig. 3-3C) at roughly every 10° of knee flexion from full extension to 90° flexion. The user was

careful to isolate the load to the medial direction of the patella as much as possible. The assessment was repeated with a lateral displacement load manually applied to the patella. Kinematic data of the femur, tibia, and patella and the orientation of the laxity instrument were collected using the Optotrak 3020 motion capture system (Northern Digital Inc., Waterloo, Canada) with data sampled at 100 Hz. Load cell feedback was displayed using Labview and sampled at 100 Hz.

#### *3.2.4 Knee Kinematic Coordinate Systems*

Tibiofemoral kinematics were described using a three-cylindrical open-chain system described by Grood and Suntay [135]. PF kinematics were described in a three-cylindrical open chain system in terms of patellar flexion, rotation, tilt, and shift (Fig. 3-4) [136]. For this study only shift and tilt motions were considered. Patellar shift is translation of the patella along the femoral ML axis with lateral as positive. Tilt is rotation of the patella about the patellar SI axis with lateral tilt (+) defined as rotation of the lateral edge of the patella toward the femur relative to the medial edge of the patella (Fig. 3-5) [136].

#### *3.2.5 Calculating PF Joint Laxity*

During each laxity assessment, the orientation of the PLI and the magnitude of the load applied to the patella were captured at 100 Hz and resolved to the directions of the patellar ML, AP, and SI axes. Patellar shift and tilt were obtained as the magnitude of the applied load reached individual load levels of 10 N, 20 N, and 30 N. Data was excluded if the medial-lateral component of the load was less than 0.7 of the entire load vector. Patellar shift and tilt during the flexion cycle with no displacement loads applied to the patella were defined as the 0 N load level. A fourth-order polynomial regression curve

was fit to the shift and tilt kinematic measurements for 0 N, 10 N, 20 N, and 30 N through the flexion range (Fig. 3-6). Patellar displacement is deviation of the patella from its neutral path with a specified load at a knee flexion angle. Excursion for 10 N was determined by finding the difference between the extracted kinematic measurements for 10 N and the kinematic measurements at 0 N through the flexion range (Fig. 3-7). The excursion measure was repeated for 20 N and 30 N of applied load. PF laxity was described as patellar excursion at a given load through the knee flexion range.

A two-way ANOVA was performed on the mean patellar shift excursion and tilt angular excursion to determine significant differences between each medial and lateral load level at knee flexion angles from 0° to 90°, in 10° increments, at a significance level of  $p = 0.05$ . An additional two-way ANOVA was performed on the mean excursions to determine differences between medial and lateral laxity under each load level at knee flexion angles, at a significance level of  $p = 0.05$ .

### *3.2.6 Principal Component Analysis*

A principal component (PC) analysis is used to reduce and explain data sets with many variables while preserving all of the variation present in the data set [137]. The data set consisted of  $p$  variables is transformed to  $p$  orthogonal and independent PCs. The first PC has the largest sample variation, the second PC contains the next largest sample variation, and so on. Generally the first few PCs contain most of the variation observed in the original variables.

PC models were developed to assess the variation in patellar laxity data through the flexion range. The model consistent of  $N$  subjects ( $N = 10$ ), with  $n$  points ( $n = 58$  for each medial and lateral excursion values from 0° to 80° knee flexion in 10° increments

for the 10, 20, and 30 N load levels and the four femoral shape measures). Let  $A$  be an  $N \times n$  matrix with each row holding the variables for one subject, and a  $n \times n$  covariance matrix,  $X$ , was found. The eigenvectors and corresponding eigenvalues of matrix  $X$  were determined and placed in matrix  $E$ , where each column held eigenvector  $e_j$ , ( $j = 1, 2, \dots, n$ ) of  $X$ . The eigenvectors are the PCs of the data. The mean of each variable was calculated and stored in  $A_{mean}$ , a  $1 \times n$  vector. The PC scores,  $P_{mean}$ , were calculated as the dot product of the PC matrix and the variables,  $P_{mean} = A_{mean}E$ .

The PC scores  $P$  were perturbed, and the resultant deformation of the variables  $A$  were calculated and graphically displayed,  $A_{perturb} = P_{perturb}E^{-1}$ , to determine the modes of variation in patellar laxity and the femoral shape measures. The shift and tilt models were perturbed by  $\pm$  two standard deviations, and the resultant deformation of the laxity and femoral shape measure variables were calculated and graphically displayed to interpret apparent variation due to each PC. The model was perturbed along a certain PC while holding all other PCs constant to represent the variation from only one PC and observing the resultant deformation in the laxity data. The interpretation was repeated for the number of PCs that cumulatively explained at least 75% of the variation in the data.

### *3.2.7 Intra-user Variability*

All the patellar laxity assessments in the study were performed by the same user, so the intra-user experimental repeatability was assessed. The same researcher performed the laxity assessments on the same specimen three times. The range of the patellar shift excursion and tilt angular excursion were calculated at every  $10^\circ$  flexion for the 10, 20, and 30 N load levels. The mean of the ranges across the knee flexion range was calculated at each load level for shift excursion and tilt rotational excursion.

### 3.3 Results

#### 3.3.1 Patellar Laxity Envelopes

A medial displacement load applied to the patella caused the patella to shift medially and tilt laterally, and a lateral load caused the patella to shift laterally and tilt medially for all the knees (Fig. 3-8). Two knees did laterally tilt in response to a lateral displacement load after at knee flexion angles greater than 30°. Generally the patellar laxity was largest at knee flexion angles of 30° or less, and laxity decreased from 30° to 90° flexion.

Maximum patellar shift excursion and tilt rotational excursion and ROM were found between 0° and 20° knee flexion, except the 30 N lateral load generated maximum shift excursion at 30° flexion and maximum tilt at 40° flexion (Table 3-1). For the 10 N load level, the maximum shift excursions were 6.1 mm medial and 4.6 mm lateral (Fig. 3-8A). The largest tilt rotational excursions under 10 N were 3.9° lateral tilt and 2.7° medial tilt (Fig. 3-8B). Patellar ROM with 10 N was at a maximum of 10.5 mm in patellar shift and 9.3° of tilt (Fig. 3-9A-B). For the 20 N load level, the largest shift excursions were 10.0 mm medial and 7.6 mm lateral, and the maximum tilt rotational excursions were 5.3° medial tilt at and 7.9° lateral tilt at. Patellar ROM at 20 N was a maximum of 17.6 mm of shift and 15.6° of patellar tilt at 20° knee flexion. The maximum patellar shift excursions with a 30 N load were 12.2 mm medially and 10.0 mm lateral. The largest tilt rotational excursions for 30 N were 7.5° medial tilt and 10.7° lateral tilt. Patellar ROM from a 30 N load on the patella was a maximum at 21.8 mm of shift and 19.3° of patellar tilt.

All three load levels were significantly different from each other in medial and lateral patellar shift and shift ROM for all flexion angles. The load levels were distinct from each other in medial tilt for all flexion angles except 90° flexion. The 10 N, 20 N, and 30 N loads were significantly different in medial tilt between full extension and 40° knee flexion. Significant differences were also found between each of the load levels in tilt ROM from 0° to 80° flexion. Overall the medial shift excursions were higher than lateral excursions; however, significant differences were only found at 0° flexion under 30 N and at 80° flexion under 20 N. Lateral tilt rotational excursions that result from a medial applied load were significantly higher than medial tilt rotational excursions from 30° to 70° knee flexion under the 20 N and 30 N loads and at 80° flexion under 20 N.

### *3.3.2 Femoral Shape Measures*

The mean EW, SA, LTS, and MTS femoral shape measures were calculated for all the knees (Table 3-1). The mean EW was 84.3 mm  $\pm$  3.3 mm and ranged from 80 mm to 90 mm. The mean SA was 134.4°  $\pm$  4.3°, ranging from 128° to 140°. The LTS and MTS were similar to one another at 22.3°  $\pm$  2.7° and 23.3°  $\pm$  4.0°, respectively.

### *3.3.3 Principal Component Analysis*

A PC analysis was performed on patellar shift excursion and tilt rotational excursion separately to determine the cause of variation in patellar laxity. The mean patellar shift laxity measures under each load level and femoral shape measures were perturbed by  $\pm$  two standard deviations along each PC and graphically displayed (Table 3-3, Fig. 3-10). The PC perturbation was repeated for the mean patellar tilt laxity envelope and femoral shape measures (Table 3-4, Fig. 3-11). The perturbation results for each PC were used to interpret variation that is accounted for in each PC (Table 3-5). In

patellar shift, the first three PCs accounted for 83% of the total variation. PC1, explaining 49.9% of variation, for both the 10 N and 30 N level was caused by specimen variation in overall shift ROM through the flexion range and the magnitude of EW and SA. PC2 (22.9% of variation) was due to the change in medial shift stiffness as the patella tracked through flexion and the amount of MTS. PC3 (10.5% of variation) was attributable to variation in medial stiffness after about 30° knee flexion and MTS. The PC analysis for patellar tilt laxity yielded three PCs that accounted for 78% of the total variation (Table 3-5). PC1 (35.0% of variation) was due to overall patellar tilt ROM at 10 N, and for 30 N was attributable to a shift in medial tilt laxity through the flexion range and an increase or decrease in lateral tilt laxity for greater than 40° knee flexion. PC1 was also attributed to EW and MTS. PC2 (29.8% of variation) was caused by tilt laxity in early flexion for a 10 N load, and the 30 N load level was due to the overall shift in lateral tilt laxity through flexion and a change in medial tilt laxity when knee flexion is less than 40°. PC2 was also attributable to inverse change in lateral and medial trochlear slope. PC3 (13.4% of variation) is caused by a change in medial tilt laxity under a 10 N load and a medialized or lateralized tilt laxity in early flexion for 30 N and the EW and MTS femoral shape measures.

#### *3.3.4 Intra-user Variability*

The intra-user experimental variation between the fitted laxity lines increased as the load applied to the patella increased (Table 3-6). The kinematic responses from a medial load (medial shift and lateral tilt) showed a larger intra-user variation than the laterally applied load. The maximum mean range for patellar shift was 2.2 mm of medial shift at 30 N and for patellar tilt was 2.4° of lateral tilt at 30 N.

### 3.4 Discussion

Patellar laxity measurements were established with the custom PLI by applying a displacement force to the patella with the PLI and recording the applied load and the resultant excursion of the patella. Distinct load levels were found through the flexion range for patellar shift and tilt laxity. Increasing the load on the patella meant an increase in shift excursion and tilt rotational excursion throughout the flexion range, but increasing the lateral load on the patella resulted in smaller tilt rotational excursions beyond 40° knee flexion where the patella is more constrained by the trochlear groove. MR images were used to quantify femoral shape measurements that contribute to patellar laxity, and a PC model correlated the variation in the femoral shape measures to the variation observed in the patellar laxity envelopes.

Although there have been studies that have measured *in vitro* patellar laxity, the current study measured laxity using a technique developed to more closely represent clinical patellar mobility tests used to evaluate patellar stability. Previous studies have measured *in vitro* laxity by applying a displacement force to the patella through a rig that attached to the anterior surface of the patella. The displacement measurements used to calculate laxity were based on the displacement of the rig and not of the patella, assuming the patellar displacement was assumed to be equal to the displacement of the rig. The current study used a motion capture system to directly measure the displacement of the patella in response to the applied load to calculate patellar laxity.

The current study was subject to a number of limitations. Any *in vitro* study can be influenced by tissue degradation through the experiment. To prevent dehydration and preserve the biomechanical quality of the soft tissue, the skin remained around the knee

joint and the knees were sprayed with a physiological saline solution. Patellar laxity was measured from a manually applied load that was not isolated in a specific direction. Clinicians use manual assessments to assess patellar stability and diagnose patellar pathologies. The user was careful to apply the displacement load in the ML direction, and to reduce the non-axial loads, forces with ML component less than 70% of the total force vector were excluded in the laxity measurements. A single 22 N quadriceps load along the femoral shaft was used to seat the patella in its neutral position but is not a physiological load. The quadriceps provide loads that have various lines of action in the coronal and sagittal planes that can apply a more complex compressive force on the patella than was represented in this study. PF contact pressure through the flexion range differs between axial quadriceps loading and multi-plane loading [31].

A manual force application was used because clinicians perform patellar mobility tests with their hands to assess a patient's patellar stability [20, 61]. Clinicians currently rely on their experience, sight, and feel when determining a patient's patellar laxity during a mobility test. The experimental method developed in this study imitates the clinical patellar mobility test. The manual load application allowed for coupled motion that naturally occurs during patellar motion. A medial displacement force caused the patella to shift medially and tilt laterally. As the patella shifted medially the lateral retinacular structures resisted the medial displacement and caused the coupled tilt motion. Simpler coupled shift and tilt motion was also observed for the medial retinaculum under lateral displacement force. The interaction of the patella with the femoral trochlear groove also contributed to the coupled motion when the patella was engaged in the groove after 20° knee flexion. When the patella shifted medially, the patella traveled up

the medial facet of the trochlear groove resulting in lateral tilt, and the patella tilted medially as it traveled up the lateral facet. Another cause of the coupled motion could be the manually applied load because the displacement force was not a pure ML force and had a compressive component. The medial displacement force would compress the medial edge of the patella into the femur and the lateral edge to lift from the femur resulting in a lateral tilt motion. The lateral displacement force also had a compressive component that resulted in medial tilt. To reduce the contribution of the compressive force to coupled motion, only displacement forces with a ML component that was 70% of the total displacement force were included in the laxity measurements.

The experimental method used in the current study to measure patellar laxity was able to capture distinct laxity load levels through the flexion range. The intra-user repeatability ranged from 0.3 mm to 1.6 mm for shift and 0.7° to 1.7° for tilt. The repeatability decreased as the displacement force increased, but the differences between the load levels were larger than the repeatability of the laxity measurement method. The error in the method itself was not likely to influence the results and assessment of the subject-to-subject variation.

The largest amount of patellar ROM occurred in early knee flexion ( $\leq 20^\circ$ ) as observed in previous studies [14-16] which found the largest amount of patellar ROM occurs in early knee flexion and decreases with flexion after 20° knee flexion. Senavongse et al. found that medial laxity of the PF joint is greater than lateral laxity throughout the flexion range [15]. The current results showed that medial and lateral shift laxities were quite similar and that medial and lateral tilt were significantly different from each other from 30° to 80° flexion. The different results can be attributed

to different quadriceps loads used. Senavongse applied a larger overall quadriceps load and distributed the load across the different heads of the quadriceps, but the current study loaded the quadriceps with a single load of 22 N along the femoral anatomical axis. Previous studies have loaded the quadriceps with a total of 175 N and reported forces of 70-240 N to generate the same patellar excursions reported in this study. Clinical studies have shown that most patients with patellar instability experience apprehension before a load application of 11 N on the patella and healthy subjects can tolerate a 22 N load with displacements between 5 mm and 13 mm [130, 132]. The current study correlated to applied load levels and displacement in the clinical studies better than previous *in vitro* studies [14-16, 127].

Patellar laxity is affected by the passive stabilization of the retinaculum, the static stabilization of the articular geometry, and the active stabilization of the quadriceps muscles. A constant quadriceps load was used for the laxity envelope assessments for all knees, so the observed variation in patellar laxity measurements and can be attributed to the stiffness of retinaculum and the articular geometry.

PC models for shift and tilt laxity were developed to assess the variation in patellar laxity and in the articular geometry. Over 78% of the variation in shift and tilt laxity was explained by the first three PCs. The variation in laxity could be contributed to the variation in soft tissue stiffness in the PF joint or the articular geometry of the distal femur and patella. The first PCs for shift and tilt were the overall ROM through the flexion range and were related to variation in EW and SA. Shift ROM increased as EW decreased and the sulcus angle increased. The increase sulcus angle provides less resistance to the patella as it displaces medially or laterally. It was expected to see that as

EW increased, shift ROM would also increase; however the opposite was found. The larger femur size correlated with a more conforming sulcus angle and may also have a stiffer retinaculum that could cause the decrease in laxity. PC1 for patellar tilt demonstrated that an increase in tilt ROM correlated with larger sulcus angle EW. The larger bone size and shallower trochlear groove provides more room for the patellar to tilt as it displaces medially or laterally.

Medial stiffness was another major mode of variation, as seen by the change in medial shift and lateral tilt stiffness in PC2 and PC3. A flatter medial trochlear facet correlated with decreased stiffness in medial shift. Only small variations in the trochlear groove measurements were found in for patellar tilt, so the change in lateral tilt stiffness through the flexion range could be attributed to the change in the stiffness in the retinaculum. The patella is not fully engaged in the trochlear groove until 20° knee flexion, the stiffness of the medial and lateral retinaculum have a higher contribution to patellar laxity than the shape of the trochlear groove.

Medial laxity showed more variation than lateral laxity beyond the first PC. Since the quadriceps force remained constant through the experiment, changes in lateral laxity could be attributed to change in quadriceps loading. A weak VMO would decrease lateral stiffness because the VMO is provided less restraint force to lateral displacement.

### 3.5 Tables and Figures

**Table 3-1: Maximum medial and lateral excursions and ROM for shift and tilt for 10 N, 20 N, and 30 N load levels.**

Load Level	Shift (mm)			Tilt (°)		
	Medial	Lateral	ROM	Medial	Lateral	ROM
10 N	6.1	4.6	10.5	2.7	3.9	9.3
20 N	10	7.6	17.6	5.3	7.9	15.6
30 N	12.2	10	21.8	7.5	10.7	19.3

**Table 3-2: Mean femoral shape measures for the ten knees that were included in the PC model.**

Femoral Shape Measure	Mean $\pm$ SD (mm)
Epicondylar Width (mm)	84.3 $\pm$ 3.3
Sulcus Angle (°)	134.4 $\pm$ 4.3
Lateral Trochlear Slope (°)	22.3 $\pm$ 2.7
Medial Trochlear Slope (°)	23.3 $\pm$ 4.0

**Table 3-3: PC perturbation results for the femoral anatomical measures in the patellar shift PC model. The mean measures were perturbed by  $\pm 2$  standard deviations along each principal component. The first three PCs explained 83.2% of the variance in the patellar shift laxity data for the ten knees.**

Anatomical Measure	Mean	PC1		PC2		PC3	
		-2SD	+2SD	-2SD	+2SD	-2SD	+2SD
Epicondylar Width (mm)	84.3	86.8	81.8	83.4	85.2	84.2	84.4
Sulcus Angle (°)	134.4	132.7	136.1	131.3	137.5	139.7	129.1
Lateral Trochlear Slope (°)	22.3	20.1	24.5	21.4	23.2	22.3	22.3
Medial Trochlear Slope (°)	23.3	27.2	19.4	27.2	19.4	18.0	28.6

**Table 3-4: PC perturbation results for the femoral anatomical measures in the patellar tilt PC model. The mean measures were perturbed by  $\pm 2$  standard deviations along each principal component. The first three PCs explained 78.1% of the variance in the patellar tilt laxity data for the ten knees.**

Anatomical Measure	Mean	PC1		PC2		PC3	
		-2SD	+2SD	-2SD	+2SD	-2SD	+2SD
Epicondylar Width (mm)	84.3	80.9	87.7	86.6	82.0	80.2	88.4
Sulcus Angle (°)	134.4	137.4	131.4	134.6	134.2	132.7	136.1
Lateral Trochlear Slope (°)	22.3	24.5	20.1	24.5	20.1	21.3	23.3
Medial Trochlear Slope (°)	23.3	18.1	28.5	21.0	25.6	26.0	20.6

**Table 3-5: PC Interpretations for patellar shift laxity PC model and tilt laxity PC model.**

	PC#	Variation	Cumulative Variation	Cause of Variation
<b>Patellar Shift</b>	1	49.9%	49.9%	Patellar shift ROM Epicondylar width and sulcus angle
	2	22.9%	72.8%	Change in medial shift stiffness through flexion range. Medial trochlear slope
	3	10.5%	83.2%	Change in medial shift stiffness after early flexion (>30°) Medial trochlear slope
<b>Patellar Tilt</b>	1	34.5%	34.5%	Patellar tilt ROM Epicondylar width and medial trochlear slope
	2	29.8%	64.8%	Change in lateral tilt stiffness through flexion. Inverse change in lateral and medial trochlear slope.
	3	13.4%	78.1%	Overall medialization or lateralization in tilt laxity in early knee flexion ( $\leq 20^\circ$ ) Epicondylar width and medial trochlear slope

**Table 3-6: The mean range of patellar shift excursion and tilt rotational excursion measures across all flexion angles at 10 N, 20 N, and 30 N load calculated from a single user performing a laxity assessment three times on the same specimen.**

Load Level	Shift (mm)		Tilt (°)	
	Medial	Lateral	Medial	Lateral
10 N	1.5	0.8	1.0	1.4
20 N	1.7	0.5	1.7	1.4
30 N	2.2	0.9	1.5	2.4

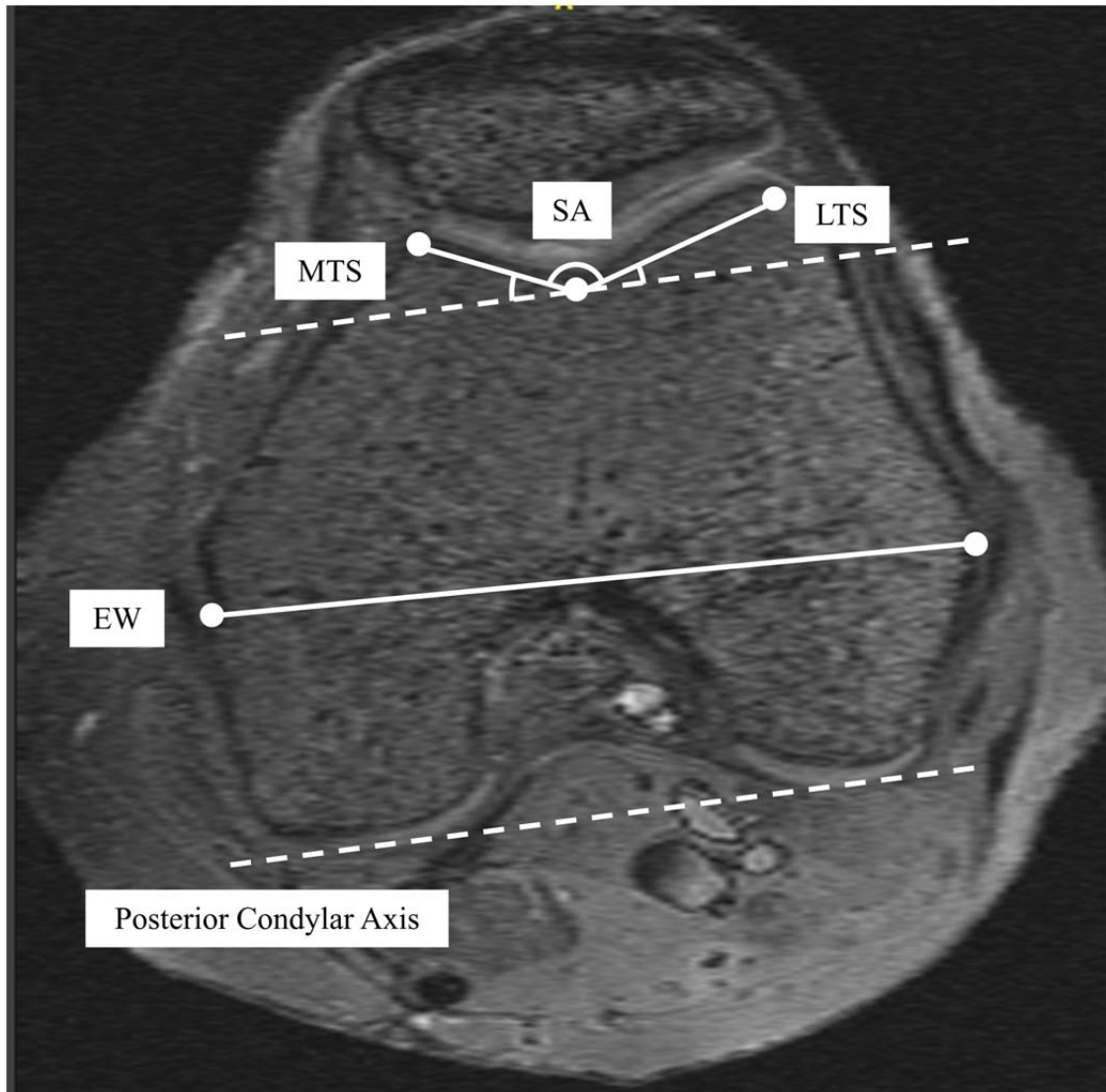


**Figure 3-1: Femoral shape measurements quantified from axial MR image. The femoral epicondylar width (EW) is the distance from the medial epicondyle to the lateral epicondyle. The medial and lateral trochlear are defined as the lines from the deepest point in the trochlear sulcus to the most anterior point of the medial and lateral bony landmarks of the trochlear groove. The sulcus angle (SA) is the angle between the medial and lateral trochlear facets. The medial trochlear slope (MTS) is the angle defined by the medial facet and the posterior condylar axis, the axis tangent to the posterior condyles (dash line). The lateral trochlear slope (LTS) is the angle between lateral facet and the posterior condylar axis.**

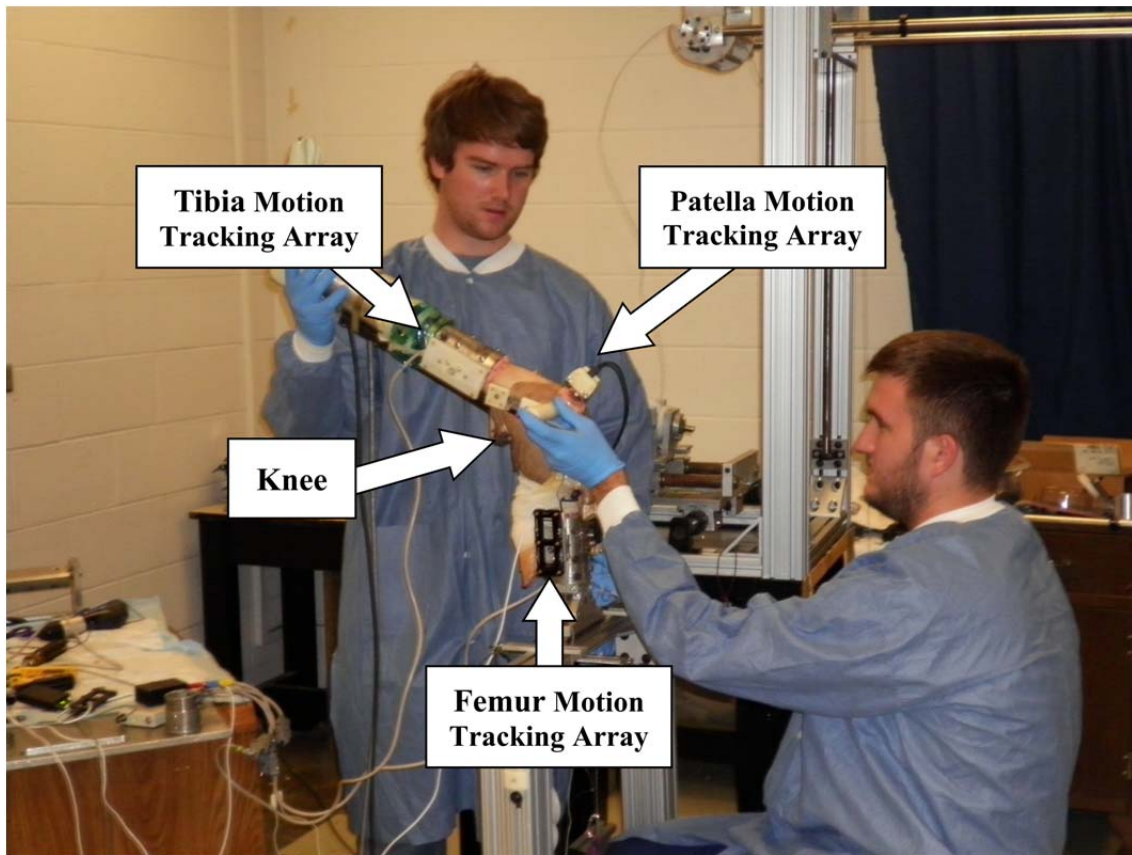


**Figure 3-2: The experimental setup of patellar laxity envelope assessment performed on the *in vitro* specimens. PF and TF kinematics were recorded through the motion tracking arrays of infrared emitting diodes attached to the femur, tibia, and patella.**

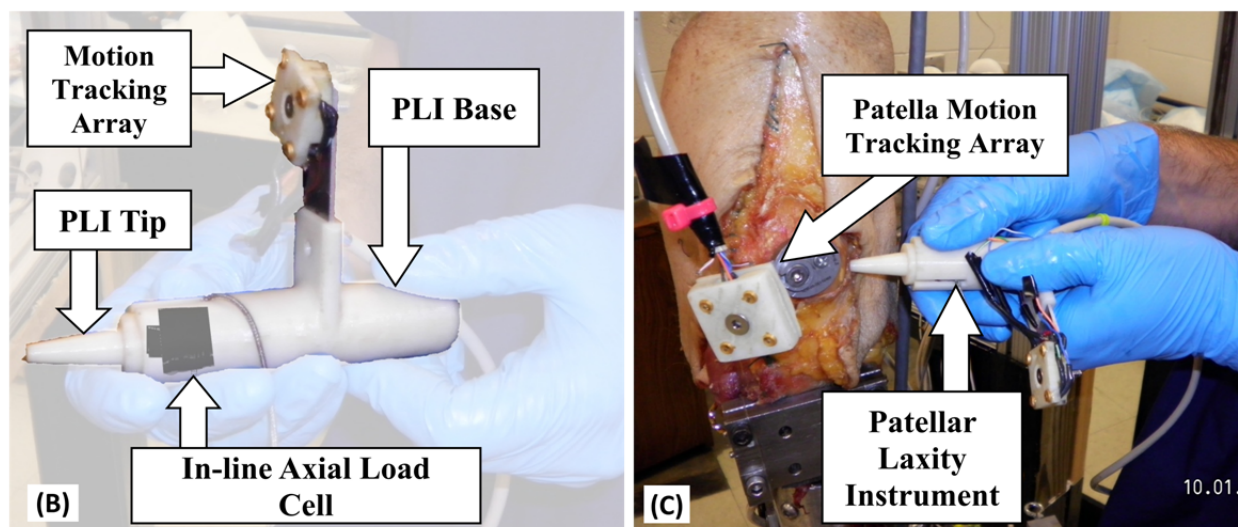
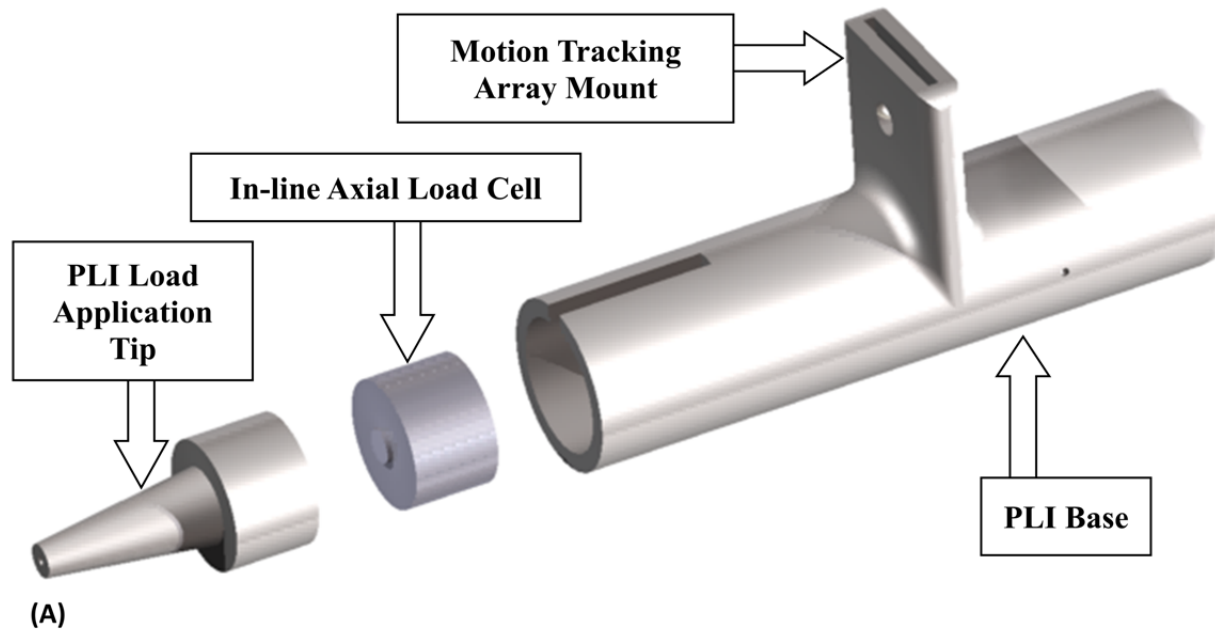


**Figure 3-3: (A) The custom PF laxity instrument (PLI) used to apply an external load on the patella at various flexion angles. (B) Loads to the patella are measured with an in-line axial load cell contained within the laxity instrument, and the direction of the load is captured through the motion tracking array mounted on the instrument. (C) The kinematic response of the patella to the applied load is measured with the motion tracking array attached to the patella.**

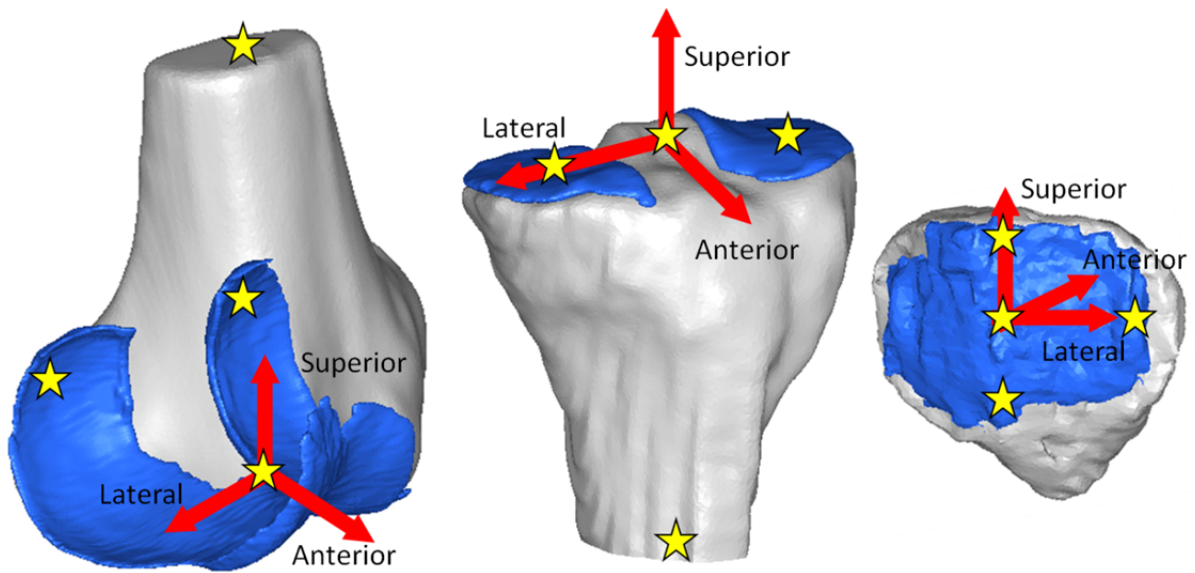


**Figure 3-4: Local bone coordinate systems were created on the femur, tibia, and patella (red arrows) using bony anatomical features on each bone (yellow stars). The most posterior points on the medial and lateral femoral condyles, the most distal point between the condyles, and the center of the femoral head were used on the femur. The centers of the medial and lateral tibial plateaus, the most proximal points between the tibial eminences, and the center of the intermedullary canal in the distal tibia.**

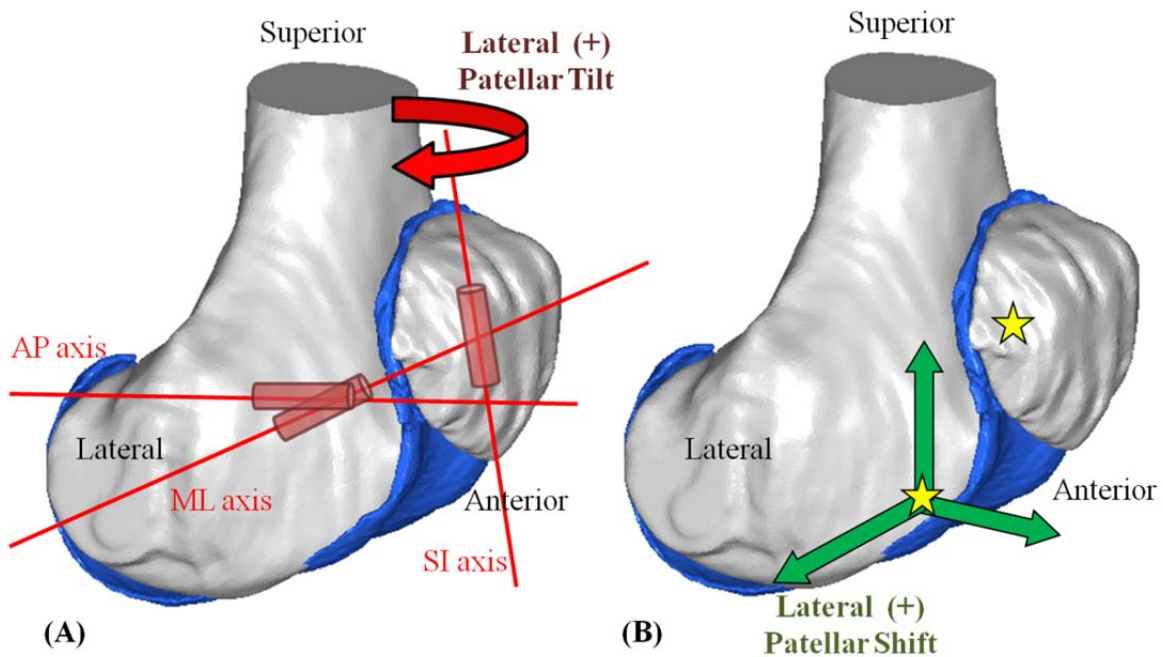


**Figure 3-5: (A) The three-cylindrical open chain system (red lines) used to calculate patellar rotations. The ML link was fixed to the femur, the SI axis was fixed to the patellar, and the AP axis was the cross product the ML and SI axes. Patellar tilt (red arrow) is rotation of the patella about the SI axis with the lateral side of the patella moving posteriorly defined as lateral (+) tilt. (B) Patellar translations are described as translation of the patellar origin relative to the femoral origin (yellow stars) along the fixed femoral coordinate system (green arrows).**

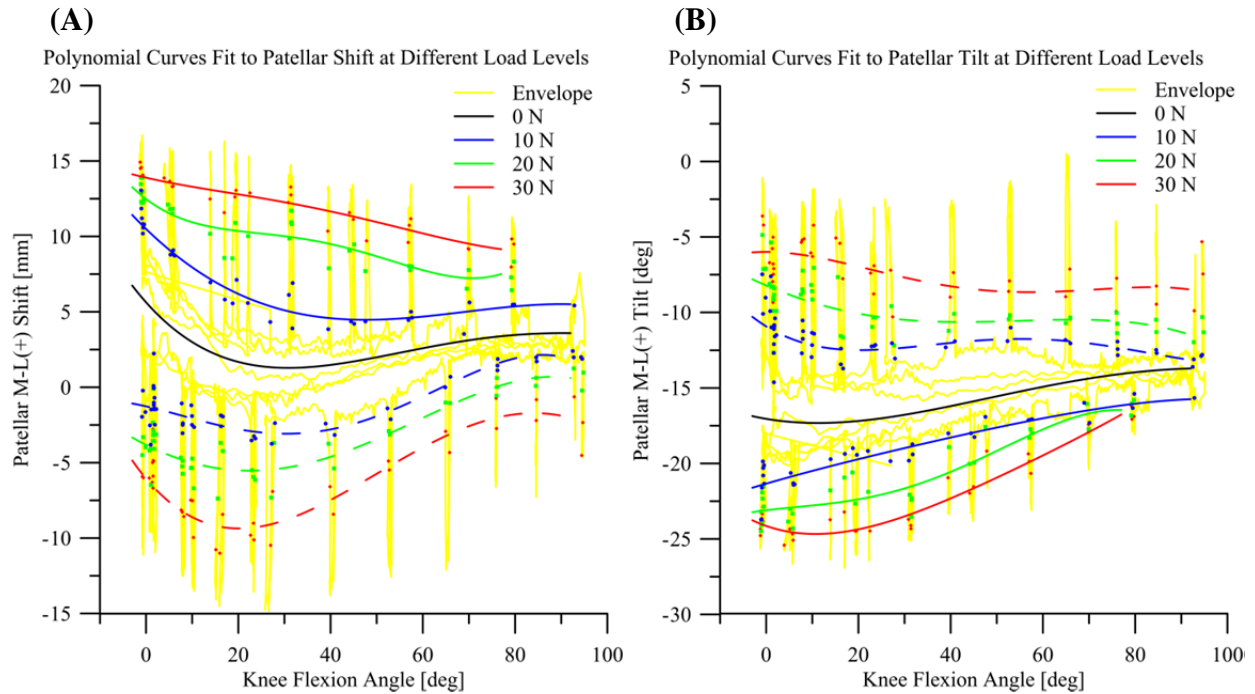


**Figure 3-6: Raw experimental patellar shift data (A) and patellar tilt data (B) (yellow) collected during PF envelope assessment for a specific specimen. Data points were extracted at different load levels (-30 N to 30 N) through the flexion range from the PFI load cell (colored points), and fourth-order polynomials were fit to the extracted data points (solid lines (lateral loads) and dash lines (medial loads)).**

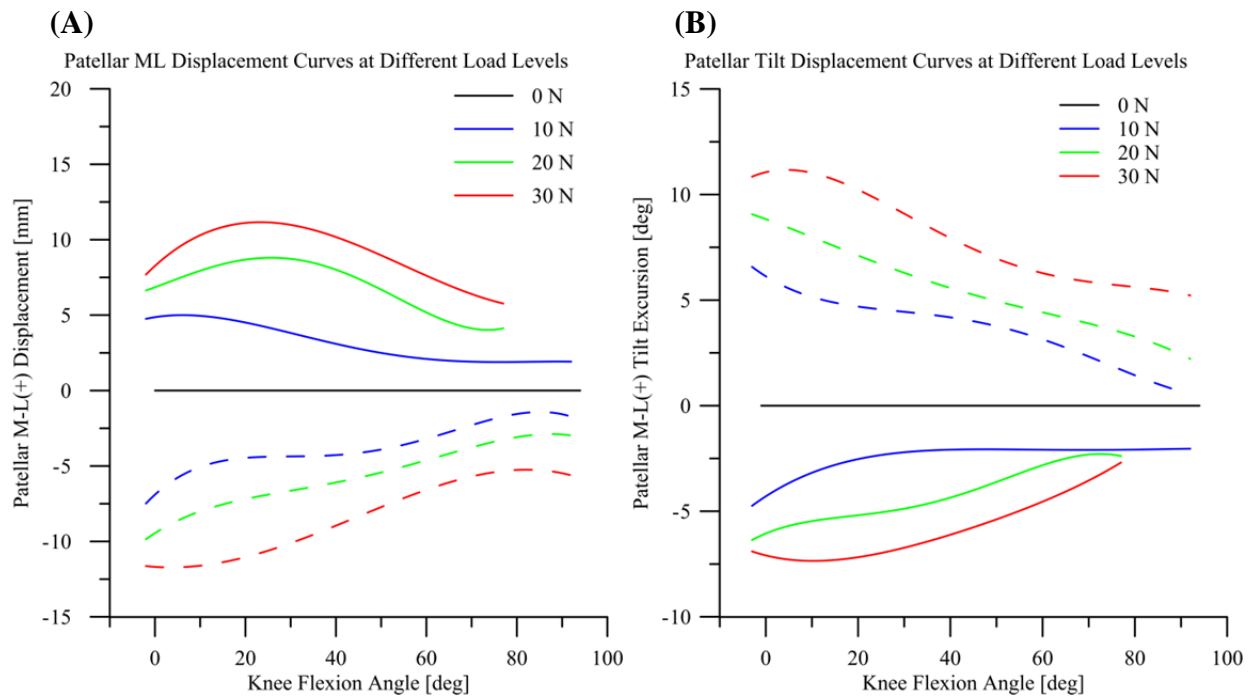


**Figure 3-7: Patellar shift (A) and patellar tilt (B) displacements were calculated from the polynomials at each load level through the flexion range for the same specimen in Fig. 3-6).**

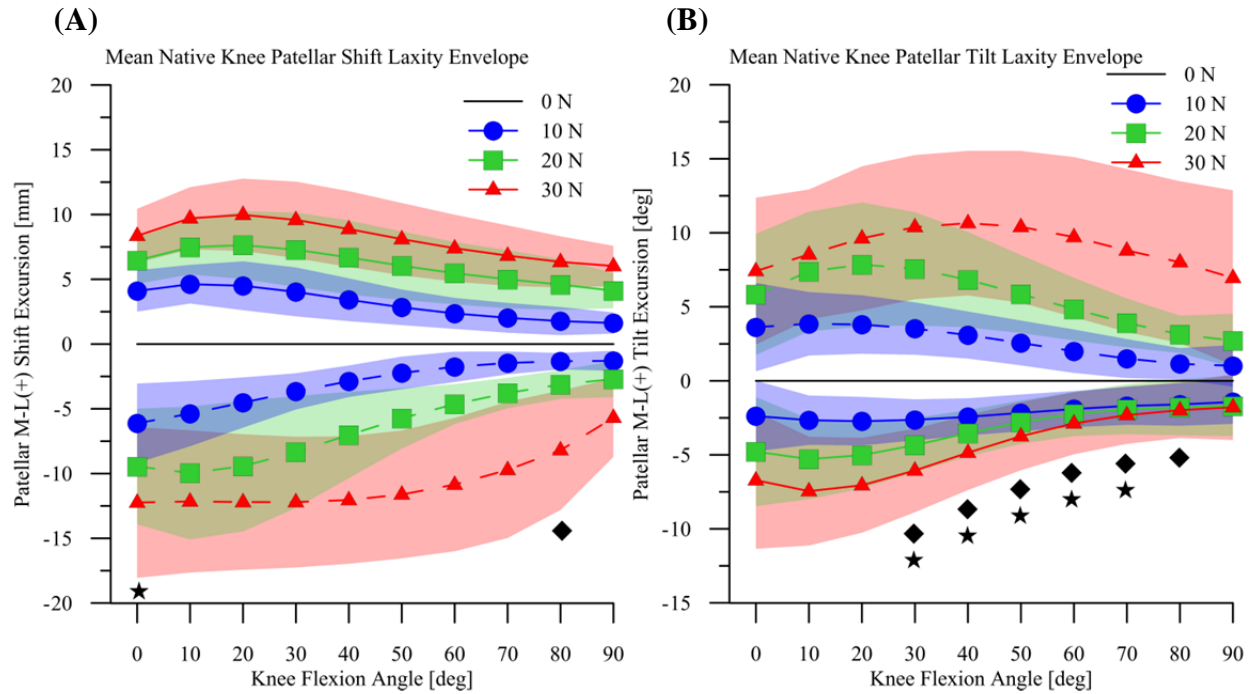


**Figure 3-8: (A) Mean patellar shift and (B) patellar tilt laxity envelopes. The shaded areas represent  $\pm 1$  standard deviation for their respective load level. No significant differences between medial and lateral patellar excursions for the 10 N load were found in shift or tilt. Flexion angles where the medial excursions differed significantly from the lateral excursions from a 20 N load (◆) and 30 N load (★) are indicated. All three load levels were significantly different from each other in medial and lateral patellar shift for all flexion angles. The load levels were distinct from each other in lateral tilt from  $0^\circ$  to  $80^\circ$ . The 10 N, 20 N, and 30 N loads were significantly different in medial tilt between full extension and  $40^\circ$  knee flexion.**

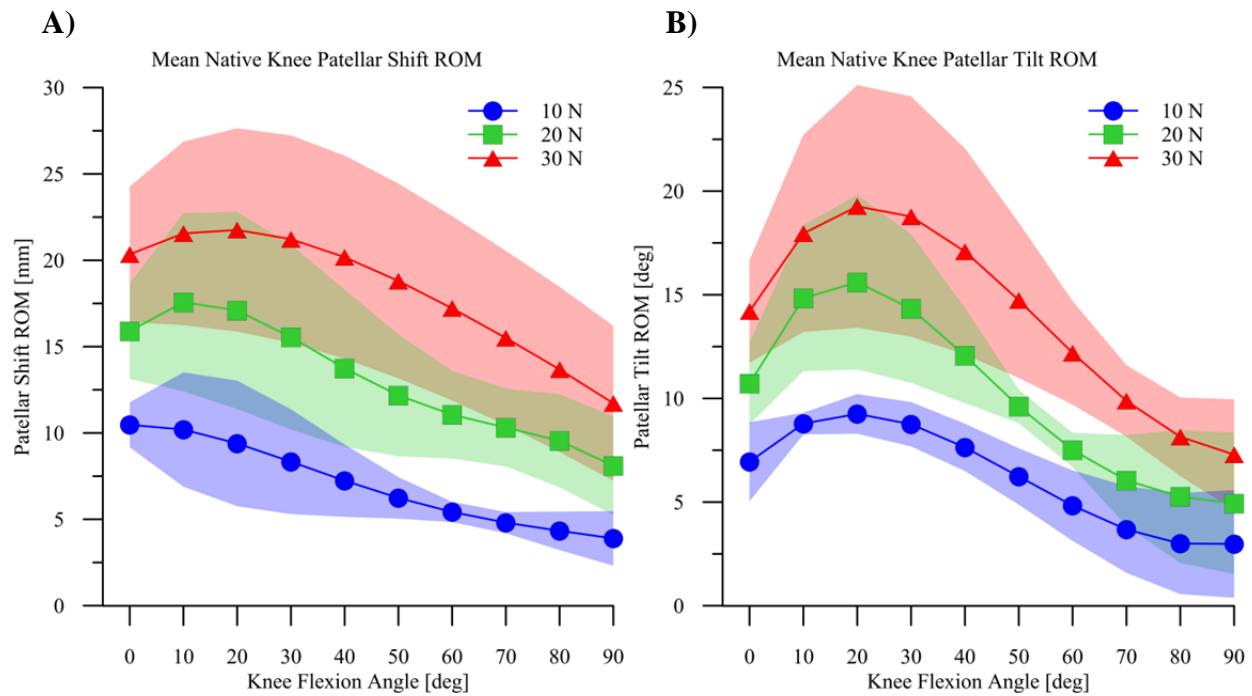


**Figure 3-9: (A) Mean patellar shift ROM and (B) mean tilt ROM under each load level with the shaded areas as  $\pm 1$  standard deviation. Significant differences were found between each of the load levels in shift ROM for all flexion angles and in tilt ROM from  $0^\circ$  to  $80^\circ$  flexion.**

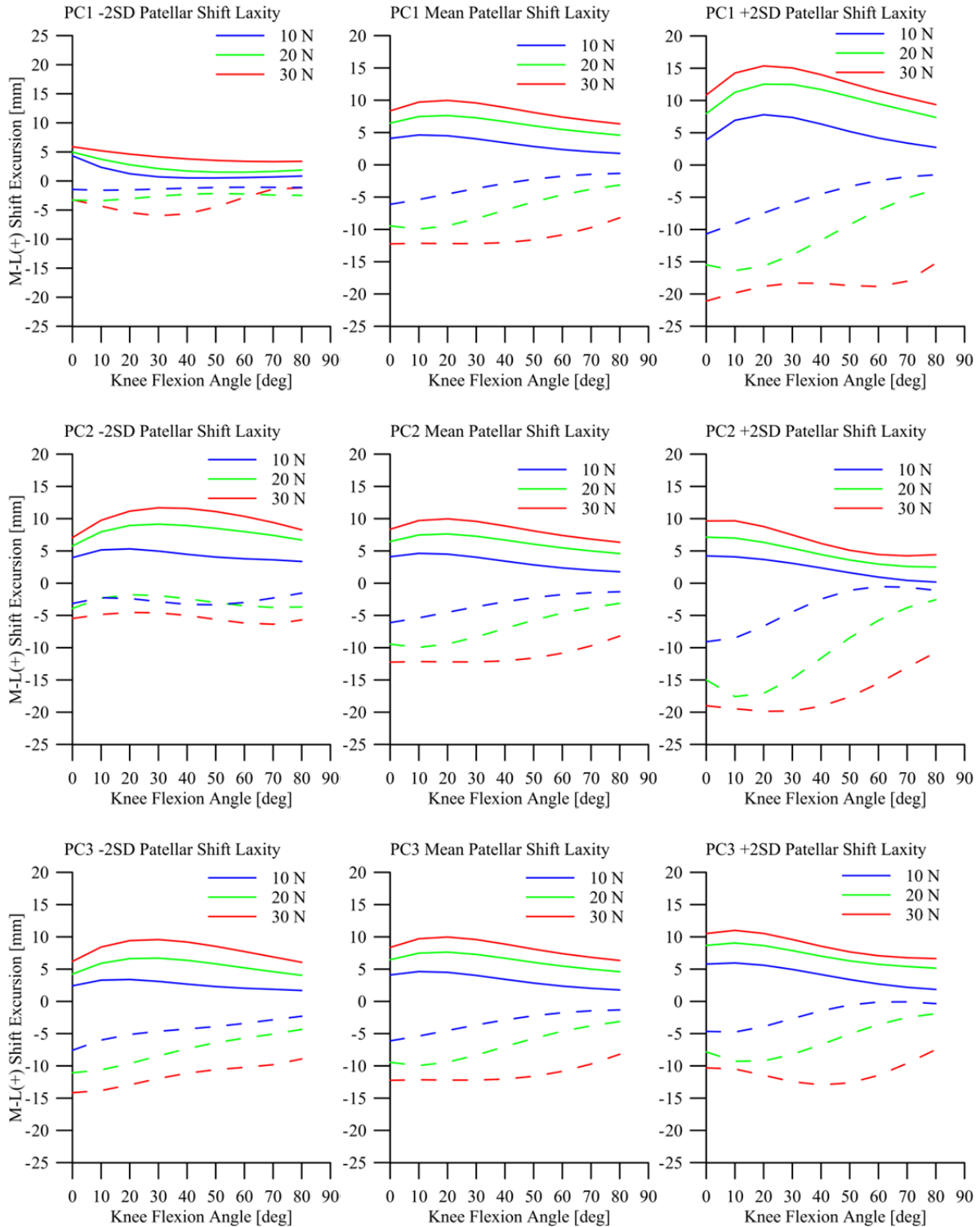


**Figure 3-10: PCA perturbation results for patellar shift laxity. The mean excursions (middle column) under  $\pm 10$  N (blue),  $\pm 20$  N (green), and  $\pm 30$  N (red) (positive loads (solid lines) and negative loads (dashed lines)) were perturbed by  $\pm 2$  standard deviations (-2SD (left column) and +2SD (right column)) along each principal component. The first three PCs explained 86.2% of the variance in the patellar shift laxity data for the ten knees.**

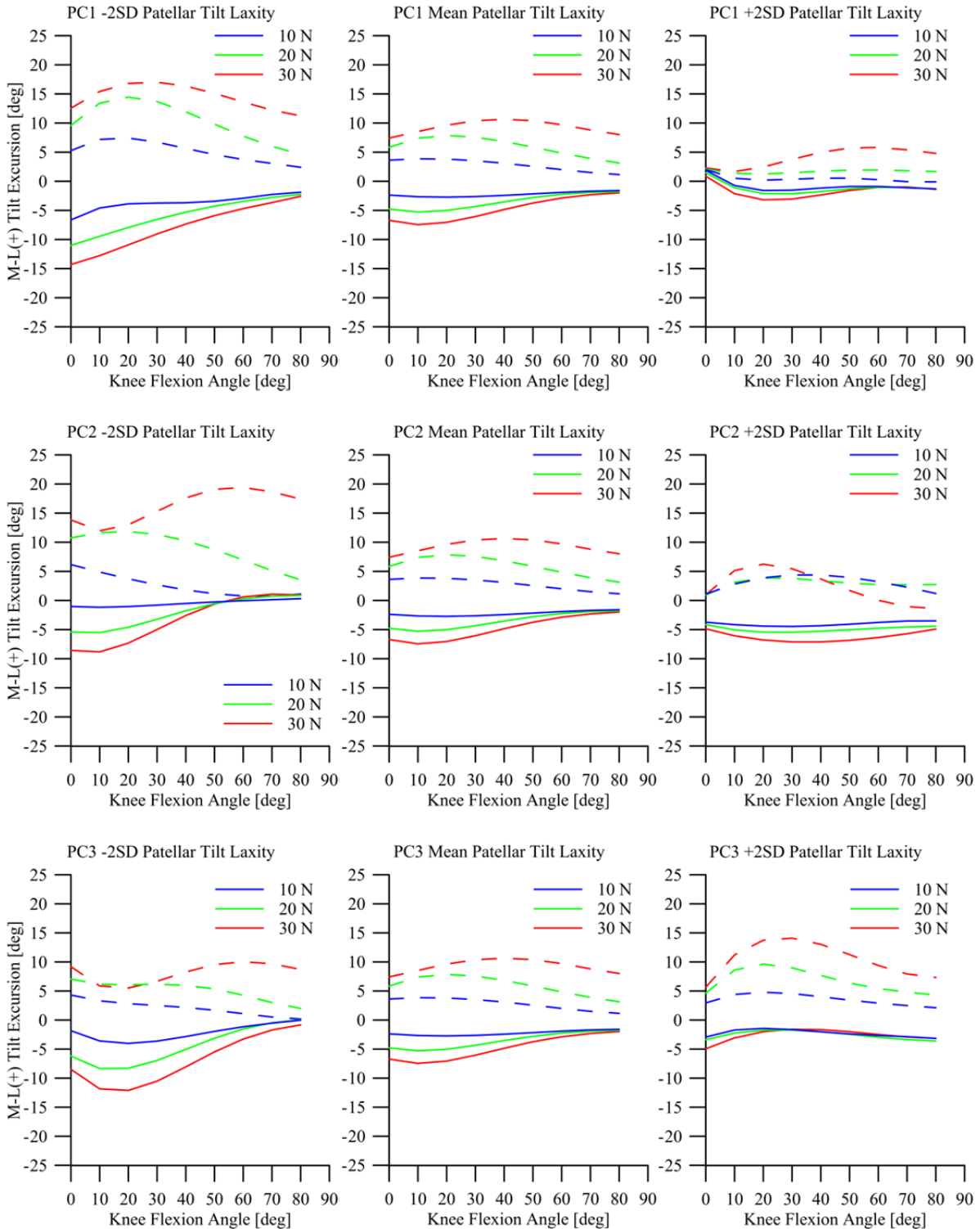


**Figure 3-11: PCA perturbation results for patellar tilt laxity. The mean excursions (middle column) under  $\pm 10$  N (blue),  $\pm 20$  N (green), and  $\pm 30$  N (red) (positive loads (solid lines) and negative loads (dashed lines)) were perturbed by  $\pm 2$  standard deviations (-2SD (left column) and +2SD (right column)) along each principal component. The first three PCs explained 80.4% of the variance in the patellar shift laxity data for the ten knees.**

## Chapter 4: Conclusions

The objective of this research is to use measure patellar laxity in the *in vitro* knee through the flexion range and to identify the types of variation in patellar laxity from subject-to-subject through the knee flexion range. Patellar laxity measurements were established with the custom PLI by applying a displacement force to the patella with the PLI and recording the applied load and the resultant excursion of the patella. Distinct load levels were found through the flexion range for patellar shift and tilt laxity. Increasing the load on the patella generally meant an increase in shift excursion and tilt rotational excursion throughout the flexion range. MR images were used to quantify femoral shape measurements that contribute to patellar laxity, and a PC model correlated the variation in the femoral shape measures to the variation observed in the patellar laxity envelopes.

Chapter 3 described experimental methods using the PLI to measured patellar laxity through the knee flexion range by applying a displacement force to the patella and measuring the applied load and the resultant displacement of the patella. A manual force application was used because clinicians perform patellar mobility tests with their hands to assess a patient's patellar stability. The manual manipulation of the patella did not restrict coupled patellar tilt and rotation that normally occurs as the patella shifts medially and laterally. The PLI demonstrated the ability to generate the patellar laxity envelope for a knee with good repeatability.

The PLI was difficult to use for first time users and required some training and practice to properly use the instrument. The application tip was free to move relative to the instrument base to indicate to the user if an off-axis load relative to the instrument's

load cell was being applied to the patella and would occasionally separate from the instrument base. The PLI design can be altered to prevent the application tip from easily separating from the instrument base. Motion tracking arrays were attached to the PLI, patella, femur, and tibia, and an Optotrak 3020 motion capture system was used to determine the orientation of the displacement force. The tracking arrays must be visible to the Optotrak cameras to capture the knee kinematic and PLI data, and with the current PLI design, the user needed to be careful to not block the tracking arrays with their hands during the envelope assessments. The envelope method and PLI could be changed to reduce the likelihood the tracking areas are blocked from the camera.

The dominant modes of variation in patellar laxity through the knee flexion range were identified using a PC analysis. Large variation in patellar laxity is present from subject-to-subject, and a PC analysis is a useful tool to understand the variation and what factors may be causing most of the variation in the data. Over 78% of the variation in shift and tilt laxity were explained by the first three PCs. Patellar laxity is affected by the passive stabilization of the retinaculum, the static stabilization of the articular geometry, and the active stabilization of the quadriceps muscles. A constant quadriceps load was used for the laxity envelope assessments for all knees, so the observed variation in patellar laxity measurements and can be attributed to the stiffness of retinaculum and the articular geometry. The largest mode of variation in patellar laxity was the overall ROM through the flexion range and was related to the variation in the femoral EW and the SA. Another cause of variation was medial of the PF joint which was affected by the steepness of the medial trochlear facet. The patella is not fully engaged in the trochlear

groove until 20° knee flexion, the stiffness of the medial and lateral retinaculum have a higher contribution to patellar laxity than the shape of the trochlear groove.

The PC model developed in Chapter 3 can have different factors included to better understand how changes in the active, passive, and static stabilizers of the PF joint correlate to variation in patellar laxity. Trochlear groove depth, individual quadriceps muscle orientations, and MPFL origin and insertion sites are some of the factors that could be included in the PC model. Overall bone size measurements of the patella and femur can be included to normalize patellar laxity data by bone size. As more subjects are added to the PC model data set, stronger correlations can be established. As more subjects are added to the PC model, it can be used to normalize data between subjects to minimize the effects of the dominant mode of variations. The results in Chapter 3 showed that PC1 accounted for over 78% of the total variation in the data set and was identified as overall laxity, or range of motion. The laxity measures could then be normalized to PC1 and remove 78% of the variation of the data, allowing other differences in the data to be more conclusively found.

The methods used in this research will be used in future research of the Experimental Joint Biomechanics Research Laboratory to measure patellar laxity with simulated pathologies that contribute patellar instability and to measure how patellar laxity changes after TKA. Component design, surgical technique, component positioning, limb alignment, balance of quadriceps extensor mechanism, component design, patellar preparation, and soft-tissue balancing are all factors that can cause change in the stabilizers of the PF joint.

## Chapter 5: References

1. Fithian, D.C., E.W. Paxton, M.L. Stone, P. Silva, D.K. Davis, D.A. Elias, and L.M. White, *Epidemiology and natural history of acute patellar dislocation*. Am J Sports Med, 2004. **32**(5): p. 1114-21.
2. Hawkins, R.J., R.H. Bell, and G. Anisette, *Acute patellar dislocations. The natural history*. Am J Sports Med, 1986. **14**(2): p. 117-20.
3. Kane, R.L., K.J. Saleh, T.J. Wilt, B. Bershadsky, W.W. Cross, 3rd, R.M. MacDonald, and I. Rutks, *Total knee replacement*. Evid Rep Technol Assess (Summ), 2003(86): p. 1-8.
4. Callahan, C.M., B.G. Drake, D.A. Heck, and R.S. Dittus, *Patient outcomes following tricompartmental total knee replacement. A meta-analysis*. JAMA, 1994. **271**(17): p. 1349-57.
5. Gioe, T.J., K.K. Killeen, K. Grimm, S. Mehle, and K. Scheltema, *Why are total knee replacements revised?: analysis of early revision in a community knee implant registry*. Clin Orthop Relat Res, 2004(428): p. 100-6.
6. Berger, R.A., L.S. Crossett, J.J. Jacobs, and H.E. Rubash, *Malrotation causing patellofemoral complications after total knee arthroplasty*. Clin Orthop Relat Res, 1998(356): p. 144-53.
7. Fehring, T.K., S. Odum, W.L. Griffin, J.B. Mason, and M. Nadaud, *Early failures in total knee arthroplasty*. Clin Orthop Relat Res, 2001(392): p. 315-8.
8. Lonner, J.H. and P.A. Lotke, *Aseptic complications after total knee arthroplasty*. J Am Acad Orthop Surg, 1999. **7**(5): p. 311-24.
9. Sharkey, P.F., W.J. Hozack, R.H. Rothman, S. Shastri, and S.M. Jacoby, *Insall Award paper. Why are total knee arthroplasties failing today?* Clin Orthop Relat Res, 2002(404): p. 7-13.
10. Barrack, R.L., A.J. Bertot, M.W. Wolfe, D.A. Waldman, M. Milicic, and L. Myers, *Patellar resurfacing in total knee arthroplasty. A prospective, randomized, double-blind study with five to seven years of follow-up*. J Bone Joint Surg Am, 2001. **83-A**(9): p. 1376-81.
11. Malo, M. and K.G. Vince, *The unstable patella after total knee arthroplasty: etiology, prevention, and management*. J Am Acad Orthop Surg, 2003. **11**(5): p. 364-71.
12. Aglietti, P., R. Buzzi, and A. Gaudenzi, *Patellofemoral functional results and complications with the posterior stabilized total condylar knee prosthesis*. J Arthroplasty, 1988. **3**(1): p. 17-25.
13. Greiwe, R.M., C. Saifi, C.S. Ahmad, and T.R. Gardner, *Anatomy and Biomechanics of Patellar Instability*. Operative Techniques in Sports Medicine, 2010. **18**(2): p. 62-67.
14. Senavongse, W. and A.A. Amis, *The effects of articular, retinacular, or muscular deficiencies on patellofemoral joint stability*. J Bone Joint Surg Br, 2005. **87**(4): p. 577-82.
15. Senavongse, W., F. Farahmand, J. Jones, H. Andersen, A.M. Bull, and A.A. Amis, *Quantitative measurement of patellofemoral joint stability: force-displacement behavior of the human patella in vitro*. J Orthop Res, 2003. **21**(5): p. 780-6.

16. Amis, A.A., C. Oguz, A.M. Bull, W. Senavongse, and D. Dejour, *The effect of trochleoplasty on patellar stability and kinematics: a biomechanical study in vitro*. J Bone Joint Surg Br, 2008. **90**(7): p. 864-9.
17. Colvin, A. and R. West, *Patellar instability*. The Journal of Bone and Joint Surgery, 2008. **90**(12): p. 2751.
18. Cofield, R.H. and R.S. Bryan, *Acute dislocation of the patella: results of conservative treatment*. J Trauma, 1977. **17**(7): p. 526-31.
19. Atkin, D.M., D.C. Fithian, K.S. Marangi, M.L. Stone, B.E. Dobson, and C. Mendelsohn, *Characteristics of patients with primary acute lateral patellar dislocation and their recovery within the first 6 months of injury*. Am J Sports Med, 2000. **28**(4): p. 472-9.
20. Ahmad, C.S., M. McCarthy, J.A. Gomez, and B.E. Shubin Stein, *The moving patellar apprehension test for lateral patellar instability*. Am J Sports Med, 2009. **37**(4): p. 791-6.
21. Nietosvaara, Y., K. Aalto, and P.E. Kallio, *Acute patellar dislocation in children: incidence and associated osteochondral fractures*. J Pediatr Orthop, 1994. **14**(4): p. 513-5.
22. Dandy, D.J., *Recurrent subluxation of the patella on extension of the knee*. J Bone Joint Surg Br, 1971. **53**(3): p. 483-7.
23. Maenpaa, H. and M.U. Lehto, *Patellar dislocation. The long-term results of nonoperative management in 100 patients*. Am J Sports Med, 1997. **25**(2): p. 213-7.
24. Amis, A.A., *Current concepts on anatomy and biomechanics of patellar stability*. Sports Med Arthrosc, 2007. **15**(2): p. 48-56.
25. Feller, J.A., A.A. Amis, J.T. Andrish, E.A. Arendt, P.J. Erasmus, and C.M. Powers, *Surgical biomechanics of the patellofemoral joint*. Arthroscopy, 2007. **23**(5): p. 542-53.
26. Holt, G., T. Nunn, R.A. Allen, A.W. Forrester, and A. Gregori, *Variation of the vastus medialis obliquus insertion and its relevance to minimally invasive total knee arthroplasty*. J Arthroplasty, 2008. **23**(4): p. 600-4.
27. Flandry, F. and G. Hommel, *Normal anatomy and biomechanics of the knee*. Sports Med Arthrosc, 2011. **19**(2): p. 82-92.
28. Farahmand, F., W. Senavongse, and A.A. Amis, *Quantitative study of the quadriceps muscles and trochlear groove geometry related to instability of the patellofemoral joint*. J Orthop Res, 1998. **16**(1): p. 136-43.
29. Bennett, W.F., N. Doherty, M.J. Hallisey, and J.P. Fulkerson, *Insertion orientation of terminal vastus lateralis obliquus and vastus medialis obliquus muscle fibers in human knees*. Clinical Anatomy, 1993. **6**(3): p. 129-134.
30. Bose, K., R. Kanagasuntherum, and M. Osman, *Vastus medialis oblique: an anatomical and physiologic study*. Orthopedics, 1980. **3**: p. 880-3.
31. Powers, C.M., J.C. Lilley, and T.Q. Lee, *The effects of axial and multi-plane loading of the extensor mechanism on the patellofemoral joint*. Clin Biomech (Bristol, Avon), 1998. **13**(8): p. 616-624.
32. Stokes, M. and A. Young, *Investigations of quadriceps inhibition: implications for clinical practice*. Physiotherapy, 1984. **70**(11): p. 425-428.

33. Grelsamer, R.P., P.M. Newton, and R.B. Staron, *The medial-lateral position of the patella on routine magnetic resonance imaging: when is normal not normal?* Arthroscopy, 1998. **14**(1): p. 23-8.
34. Goh, J.C., P.Y. Lee, and K. Bose, *A cadaver study of the function of the oblique part of vastus medialis.* J Bone Joint Surg Br, 1995. **77**(2): p. 225-31.
35. Panagiotopoulos, E., P. Strzelczyk, M. Herrmann, and G. Scuderi, *Cadaveric study on static medial patellar stabilizers: the dynamizing role of the vastus medialis obliquus on medial patellofemoral ligament.* Knee Surg Sports Traumatol Arthrosc, 2006. **14**(1): p. 7-12.
36. Sallay, P.I., J. Poggi, K.P. Speer, and W.E. Garrett, *Acute dislocation of the patella. A correlative pathoanatomic study.* Am J Sports Med, 1996. **24**(1): p. 52-60.
37. Powers, C.M., *Rehabilitation of patellofemoral joint disorders: a critical review.* J Orthop Sports Phys Ther, 1998. **28**(5): p. 345-54.
38. Cowan, S.M., K.L. Bennell, and P.W. Hodges, *Therapeutic patellar taping changes the timing of vasti muscle activation in people with patellofemoral pain syndrome.* Clin J Sport Med, 2002. **12**(6): p. 339-47.
39. McConnell, J., *Rehabilitation and nonoperative treatment of patellar instability.* Sports Med Arthrosc, 2007. **15**(2): p. 95-104.
40. Hunter, S.C., R. Marascalco, and J.C. Hughston, *Disruption of the vastus medialis obliquus with medial knee ligament injuries.* The American Journal of Sports Medicine, 1983. **11**(6): p. 427.
41. Ahmad, C.S., B.E. Stein, D. Matuz, and J.H. Henry, *Immediate surgical repair of the medial patellar stabilizers for acute patellar dislocation. A review of eight cases.* Am J Sports Med, 2000. **28**(6): p. 804-10.
42. Garth, W.P., Jr., D.G. DiChristina, and G. Holt, *Delayed proximal repair and distal realignment after patellar dislocation.* Clin Orthop Relat Res, 2000(377): p. 132-44.
43. Conlan, T., W.P. Garth, Jr., and J.E. Lemons, *Evaluation of the medial soft-tissue restraints of the extensor mechanism of the knee.* J Bone Joint Surg Am, 1993. **75**(5): p. 682-93.
44. Desio, S.M., R.T. Burks, and K.N. Bachus, *Soft tissue restraints to lateral patellar translation in the human knee.* Am J Sports Med, 1998. **26**(1): p. 59-65.
45. Hautamaa, P.V., D.C. Fithian, K.R. Kaufman, D.M. Daniel, and A.M. Pohlmeier, *Medial soft tissue restraints in lateral patellar instability and repair.* Clin Orthop Relat Res, 1998(349): p. 174-82.
46. Nomura, E., Y. Horiuchi, and M. Kihara, *Medial patellofemoral ligament restraint in lateral patellar translation and reconstruction.* Knee, 2000. **7**(2): p. 121-127.
47. Burks, R.T., S.M. Desio, K.N. Bachus, L. Tyson, and K. Springer, *Biomechanical evaluation of lateral patellar dislocations.* Am J Knee Surg, 1998. **11**(1): p. 24-31.
48. Warren, L.F. and J.L. Marshall, *The supporting structures and layers on the medial side of the knee: an anatomical analysis.* J Bone Joint Surg Am, 1979. **61**(1): p. 56-62.

49. Feller, J.A., J.A. Feagin, Jr., and W.E. Garrett, Jr., *The medial patellofemoral ligament revisited: an anatomical study*. Knee Surg Sports Traumatol Arthrosc, 1993. **1**(3-4): p. 184-6.
50. LaPrade, R.F., A.H. Engebretsen, T.V. Ly, S. Johansen, F.A. Wentorf, and L. Engebretsen, *The anatomy of the medial part of the knee*. J Bone Joint Surg Am, 2007. **89**(9): p. 2000-10.
51. Baldwin, J.L., *The anatomy of the medial patellofemoral ligament*. Am J Sports Med, 2009. **37**(12): p. 2355-61.
52. Balcarek, P., J. Ammon, S. Frosch, T.A. Walde, J.P. Schuttrumpf, K.G. Ferlemann, H. Lill, K.M. Sturmer, and K.H. Frosch, *Magnetic resonance imaging characteristics of the medial patellofemoral ligament lesion in acute lateral patellar dislocations considering trochlear dysplasia, patella alta, and tibial tuberosity-trochlear groove distance*. Arthroscopy, 2010. **26**(7): p. 926-35.
53. Fulkerson, J.P. and H.R. Gossling, *Anatomy of the knee joint lateral retinaculum*. Clin Orthop Relat Res, 1980(153): p. 183-8.
54. Terry, G.C., J.C. Hughston, and L.A. Norwood, *The anatomy of the iliopatellar band and iliotibial tract*. Am J Sports Med, 1986. **14**(1): p. 39-45.
55. Kaplan, E.B., *Surgical approach to the lateral (peroneal) side of the knee joint*. Surg Gynecol Obstet, 1957. **104**(3): p. 346-56.
56. Kwak, S.D., C.S. Ahmad, T.R. Gardner, R.P. Grelsamer, J.H. Henry, L. Blankevoort, G.A. Ateshian, and V.C. Mow, *Hamstrings and iliotibial band forces affect knee kinematics and contact pattern*. J Orthop Res, 2000. **18**(1): p. 101-8.
57. Merican, A.M. and A.A. Amis, *Iliotibial band tension affects patellofemoral and tibiofemoral kinematics*. J Biomech, 2009. **42**(10): p. 1539-46.
58. Merican, A.M., F. Iranpour, and A.A. Amis, *Iliotibial band tension reduces patellar lateral stability*. J Orthop Res, 2009. **27**(3): p. 335-9.
59. Fredericson, M. and C.M. Powers, *Practical management of patellofemoral pain*. Clin J Sport Med, 2002. **12**(1): p. 36-8.
60. Merican, A.M., E. Kondo, and A.A. Amis, *The effect on patellofemoral joint stability of selective cutting of lateral retinacular and capsular structures*. J Biomech, 2009. **42**(3): p. 291-6.
61. Kolowich, P.A., L.E. Paulos, T.D. Rosenberg, and S. Farnsworth, *Lateral release of the patella: indications and contraindications*. Am J Sports Med, 1990. **18**(4): p. 359-65.
62. Lattermann, C., J. Toth, and B.R. Bach, Jr., *The role of lateral retinacular release in the treatment of patellar instability*. Sports Med Arthrosc, 2007. **15**(2): p. 57-60.
63. Fulkerson, J.P., *Diagnosis and treatment of patients with patellofemoral pain*. Am J Sports Med, 2002. **30**(3): p. 447-56.
64. Nam, E.K. and R.P. Karzel, *Mini-open medial reefing and arthroscopic lateral release for the treatment of recurrent patellar dislocation: a medium-term follow-up*. Am J Sports Med, 2005. **33**(2): p. 220-30.
65. Ali, S. and A. Bhatti, *Arthroscopic proximal realignment of the patella for recurrent instability: report of a new surgical technique with 1 to 7 years of follow-up*. Arthroscopy, 2007. **23**(3): p. 305-11.

66. Nikku, R., Y. Nietosvaara, P.E. Kallio, K. Aalto, and J.E. Michelsson, *Operative versus closed treatment of primary dislocation of the patella. Similar 2-year results in 125 randomized patients.* Acta Orthop Scand, 1997. **68**(5): p. 419-23.
67. Nikku, R., Y. Nietosvaara, K. Aalto, and P.E. Kallio, *Operative treatment of primary patellar dislocation does not improve medium-term outcome: A 7-year follow-up report and risk analysis of 127 randomized patients.* Acta Orthop, 2005. **76**(5): p. 699-704.
68. Steiner, T.M., R. Torga-Spak, and R.A. Teitge, *Medial patellofemoral ligament reconstruction in patients with lateral patellar instability and trochlear dysplasia.* Am J Sports Med, 2006. **34**(8): p. 1254-61.
69. Elias, J.J. and A.J. Cosgarea, *Technical errors during medial patellofemoral ligament reconstruction could overload medial patellofemoral cartilage: a computational analysis.* Am J Sports Med, 2006. **34**(9): p. 1478-85.
70. Panagopoulos, A., L. van Niekerk, and I.K. Triantafillopoulos, *MPFL reconstruction for recurrent patella dislocation: a new surgical technique and review of the literature.* Int J Sports Med, 2008. **29**(5): p. 359-65.
71. Mikashima, Y., M. Kimura, Y. Kobayashi, M. Miyawaki, and T. Tomatsu, *Clinical results of isolated reconstruction of the medial patellofemoral ligament for recurrent dislocation and subluxation of the patella.* Acta Orthop Belg, 2006. **72**(1): p. 65-71.
72. Nomura, E. and M. Inoue, *Hybrid medial patellofemoral ligament reconstruction using the semitendinous tendon for recurrent patellar dislocation: minimum 3 years' follow-up.* Arthroscopy, 2006. **22**(7): p. 787-93.
73. Ahmed, A.M. and N.A. Duncan, *Correlation of patellar tracking pattern with trochlear and retropatellar surface topographies.* J Biomech Eng, 2000. **122**(6): p. 652-60.
74. Jafaril, A., F. Farahmand, and A. Meghdari, *The effects of trochlear groove geometry on patellofemoral joint stability--a computer model study.* Proc Inst Mech Eng H, 2008. **222**(1): p. 75-88.
75. Carrillon, Y., H. Abidi, D. Dejour, O. Fantino, B. Moyon, and V.A. Tran-Minh, *Patellar instability: assessment on MR images by measuring the lateral trochlear inclination-initial experience.* Radiology, 2000. **216**(2): p. 582-5.
76. Shih, Y.F., A.M. Bull, and A.A. Amis, *The cartilaginous and osseous geometry of the femoral trochlear groove.* Knee Surg Sports Traumatol Arthrosc, 2004. **12**(4): p. 300-6.
77. Kalichman, L., Y. Zhu, Y. Zhang, J. Niu, D. Gale, D.T. Felson, and D. Hunter, *The association between patella alignment and knee pain and function: an MRI study in persons with symptomatic knee osteoarthritis.* Osteoarthritis Cartilage, 2007. **15**(11): p. 1235-40.
78. Merchant, A.C., R.L. Mercer, R.H. Jacobsen, and C.R. Cool, *Roentgenographic analysis of patellofemoral congruence.* J Bone Joint Surg Am, 1974. **56**(7): p. 1391-6.
79. Bollier, M. and J.P. Fulkerson, *The role of trochlear dysplasia in patellofemoral instability.* J Am Acad Orthop Surg, 2011. **19**(1): p. 8-16.
80. Lee, T.Q., B.Y. Yang, M.D. Sandusky, and P.J. McMahon, *The effects of tibial rotation on the patellofemoral joint: assessment of the changes in in situ strain in*

- the peripatellar retinaculum and the patellofemoral contact pressures and areas.* J Rehabil Res Dev, 2001. **38**(5): p. 463-9.
81. Dejour, H., G. Walch, L. Nove-Josserand, and C. Guier, *Factors of patellar instability: an anatomic radiographic study.* Knee Surg Sports Traumatol Arthrosc, 1994. **2**(1): p. 19-26.
  82. Dejour, D. and B. Le Coultre, *Osteotomies in patello-femoral instabilities.* Sports Med Arthrosc, 2007. **15**(1): p. 39-46.
  83. Maenpaa, H. and M.U. Lehto, *Patellar dislocation has predisposing factors. A roentgenographic study on lateral and tangential views in patients and healthy controls.* Knee Surg Sports Traumatol Arthrosc, 1996. **4**(4): p. 212-6.
  84. Davies-Tuck, M., A.J. Teichtahl, A.E. Wluka, Y. Wang, D.M. Urquhart, J. Cui, and F.M. Cicuttini, *Femoral sulcus angle and increased patella facet cartilage volume in an osteoarthritic population.* Osteoarthritis Cartilage, 2008. **16**(1): p. 131-5.
  85. Verdonk, R., E. Jansegers, and B. Stuyts, *Trochleoplasty in dysplastic knee trochlea.* Knee Surg Sports Traumatol Arthrosc, 2005. **13**(7): p. 529-33.
  86. Albee, F.H., *The Bone Graft Peg in the Treatment of Fractures of Neck of Femur: Author's Technic.* Ann Surg, 1915. **62**(1): p. 85-91.
  87. Schottle, P.B., S.F. Fucentese, C. Pfirrmann, H. Bereiter, and J. Romero, *Trochleaplasty for patellar instability due to trochlear dysplasia: A minimum 2-year clinical and radiological follow-up of 19 knees.* Acta Orthop, 2005. **76**(5): p. 693-8.
  88. Bicos, J., J.P. Fulkerson, and A. Amis, *Current concepts review: the medial patellofemoral ligament.* Am J Sports Med, 2007. **35**(3): p. 484-92.
  89. Rhoads, D.D., P.C. Noble, J.D. Reuben, O.M. Mahoney, and H.S. Tullos, *The effect of femoral component position on patellar tracking after total knee arthroplasty.* Clin Orthop Relat Res, 1990(260): p. 43-51.
  90. Healy, W.L., S.A. Wasilewski, R. Takei, and M. Oberlander, *Patellofemoral complications following total knee arthroplasty. Correlation with implant design and patient risk factors.* J Arthroplasty, 1995. **10**(2): p. 197-201.
  91. Merkow, R.L., M. Soudry, and J.N. Insall, *Patellar dislocation following total knee replacement.* J Bone Joint Surg Am, 1985. **67**(9): p. 1321-7.
  92. Akagi, M., Y. Matsusue, T. Mata, Y. Asada, M. Horiguchi, H. Iida, and T. Nakamura, *Effect of rotational alignment on patellar tracking in total knee arthroplasty.* Clin Orthop Relat Res, 1999(366): p. 155-63.
  93. Anouchi, Y.S., L.A. Whiteside, A.D. Kaiser, and M.T. Milliano, *The effects of axial rotational alignment of the femoral component on knee stability and patellar tracking in total knee arthroplasty demonstrated on autopsy specimens.* Clin Orthop Relat Res, 1993(287): p. 170-7.
  94. Kelly, M.A., *Patellofemoral complications following total knee arthroplasty.* Instr Course Lect, 2001. **50**: p. 403-7.
  95. Briard, J.L. and D.S. Hungerford, *Patellofemoral instability in total knee arthroplasty.* J Arthroplasty, 1989. **4 Suppl**: p. S87-97.
  96. Nagamine, R., L.A. Whiteside, S.E. White, and D.S. McCarthy, *Patellar tracking after total knee arthroplasty. The effect of tibial tray malrotation and articular surface configuration.* Clin Orthop Relat Res, 1994(304): p. 262-71.

97. Rhoads, D.D., P.C. Noble, J.D. Reuben, and H.S. Tullos, *The effect of femoral component position on the kinematics of total knee arthroplasty*. Clin Orthop Relat Res, 1993(286): p. 122-9.
98. Yoshii, I., L.A. Whiteside, and Y.S. Anouchi, *The effect of patellar button placement and femoral component design on patellar tracking in total knee arthroplasty*. Clin Orthop Relat Res, 1992(275): p. 211-9.
99. Schroer, W.C., P.J. Diesfeld, M.E. Reedy, and A.R. LeMarr, *Isokinetic strength testing of minimally invasive total knee arthroplasty recovery*. J Arthroplasty, 2010. **25**(2): p. 274-9.
100. Hofmann, A.A., R.L. Plaster, and L.E. Murdock, *Subvastus (Southern) approach for primary total knee arthroplasty*. Clin Orthop Relat Res, 1991(269): p. 70-7.
101. Tashiro, Y., H. Miura, S. Matsuda, K. Okazaki, and Y. Iwamoto, *Minimally invasive versus standard approach in total knee arthroplasty*. Clin Orthop Relat Res, 2007. **463**: p. 144-50.
102. Enis, J.E., R. Gardner, M.A. Robledo, L. Latta, and R. Smith, *Comparison of patellar resurfacing versus nonresurfacing in bilateral total knee arthroplasty*. Clin Orthop Relat Res, 1990(260): p. 38-42.
103. Keblish, P.A., A.K. Varma, and A.S. Greenwald, *Patellar resurfacing or retention in total knee arthroplasty. A prospective study of patients with bilateral replacements*. J Bone Joint Surg Br, 1994. **76**(6): p. 930-7.
104. Bourne, R.B., C.H. Rorabeck, M. Vaz, J. Kramer, R. Hardie, and D. Robertson, *Resurfacing versus not resurfacing the patella during total knee replacement*. Clin Orthop Relat Res, 1995(321): p. 156-61.
105. Feller, J.A., R.J. Bartlett, and D.M. Lang, *Patellar resurfacing versus retention in total knee arthroplasty*. J Bone Joint Surg Br, 1996. **78**(2): p. 226-8.
106. Wood, D.J., A.J. Smith, D. Collopy, B. White, B. Brankov, and M.K. Bulsara, *Patellar resurfacing in total knee arthroplasty: a prospective, randomized trial*. J Bone Joint Surg Am, 2002. **84-A**(2): p. 187-93.
107. Waters, T.S. and G. Bentley, *Patellar resurfacing in total knee arthroplasty. A prospective, randomized study*. J Bone Joint Surg Am, 2003. **85-A**(2): p. 212-7.
108. Campbell, D.G., W.W. Duncan, M. Ashworth, A. Mintz, J. Stirling, L. Wakefield, and T.M. Stevenson, *Patellar resurfacing in total knee replacement: a ten-year randomised prospective trial*. J Bone Joint Surg Br, 2006. **88**(6): p. 734-9.
109. Myles, C.M., P.J. Rowe, R.W. Nutton, and R. Burnett, *The effect of patella resurfacing in total knee arthroplasty on functional range of movement measured by flexible electrogoniometry*. Clin Biomech (Bristol, Avon), 2006. **21**(7): p. 733-9.
110. Burnett, R.S., J.L. Boone, K.P. McCarthy, S. Rosenzweig, and R.L. Barrack, *A prospective randomized clinical trial of patellar resurfacing and nonresurfacing in bilateral TKA*. Clin Orthop Relat Res, 2007. **464**: p. 65-72.
111. Smith, A.J., D.J. Wood, and M.G. Li, *Total knee replacement with and without patellar resurfacing: a prospective, randomised trial using the profix total knee system*. J Bone Joint Surg Br, 2008. **90**(1): p. 43-9.
112. Conditt, M.A., P.C. Noble, B. Allen, M. Shen, B.S. Parsley, and K.B. Mathis, *Surface damage of patellar components used in total knee arthroplasty*. J Bone Joint Surg Am, 2005. **87**(6): p. 1265-71.

113. Insall, J., V. Goldberg, and E. Salvati, *Recurrent dislocation and the high-riding patella*. Clin Orthop Relat Res, 1972. **88**: p. 67-9.
114. Lancourt, J.E. and J.A. Cristini, *Patella alta and patella infera. Their etiological role in patellar dislocation, chondromalacia, and apophysitis of the tibial tubercle*. J Bone Joint Surg Am, 1975. **57**(8): p. 1112-5.
115. Kannus, P.A., *Long patellar tendon: radiographic sign of patellofemoral pain syndrome--a prospective study*. Radiology, 1992. **185**(3): p. 859-63.
116. Aglietti, P., J.N. Insall, and G. Cerulli, *Patellar pain and incongruence. I: Measurements of incongruence*. Clin Orthop Relat Res, 1983(176): p. 217-24.
117. Laurin, C.A., R. Dussault, and H.P. Levesque, *The tangential x-ray investigation of the patellofemoral joint: x-ray technique, diagnostic criteria and their interpretation*. Clin Orthop Relat Res, 1979(144): p. 16-26.
118. Laurin, C.A., H.P. Levesque, R. Dussault, H. Labelle, and J.P. Peides, *The abnormal lateral patellofemoral angle: a diagnostic roentgenographic sign of recurrent patellar subluxation*. J Bone Joint Surg Am, 1978. **60**(1): p. 55-60.
119. Haim, A., M. Yaniv, S. Dekel, and H. Amir, *Patellofemoral pain syndrome: validity of clinical and radiological features*. Clin Orthop Relat Res, 2006. **451**: p. 223-8.
120. Sanders, T.G., W.B. Morrison, B.A. Singleton, M.D. Miller, and K.G. Cornum, *Medial patellofemoral ligament injury following acute transient dislocation of the patella: MR findings with surgical correlation in 14 patients*. J Comput Assist Tomogr, 2001. **25**(6): p. 957-62.
121. Elias, D.A., L.M. White, and D.C. Fithian, *Acute lateral patellar dislocation at MR imaging: injury patterns of medial patellar soft-tissue restraints and osteochondral injuries of the inferomedial patella*. Radiology, 2002. **225**(3): p. 736-43.
122. Harbaugh, C.M., N.A. Wilson, and F.T. Sheehan, *Correlating femoral shape with patellar kinematics in patients with patellofemoral pain*. J Orthop Res, 2010. **28**(7): p. 865-72.
123. Collado, H. and M. Fredericson, *Patellofemoral pain syndrome*. Clin Sports Med, 2010. **29**(3): p. 379-98.
124. Galway, H.R. and D.L. MacIntosh, *The lateral pivot shift: a symptom and sign of anterior cruciate ligament insufficiency*. Clin Orthop Relat Res, 1980(147): p. 45-50.
125. Matsen, F.A. and C.A. Rockwood, *Anterior glenohumeral instability*, in *The Shoulder*, C.A. Rockwood and F.A. Matsen, Editors. 1990, Saunders: Philadelphia. p. 526-622.
126. O'Driscoll, S.W., R.L. Lawton, and A.M. Smith, *The "moving valgus stress test" for medial collateral ligament tears of the elbow*. Am J Sports Med, 2005. **33**(2): p. 231-9.
127. Farahmand, F., M.N. Tahmasbi, and A.A. Amis, *Lateral force-displacement behaviour of the human patella and its variation with knee flexion--a biomechanical study in vitro*. J Biomech, 1998. **31**(12): p. 1147-52.
128. Teitge, R.A., W.W. Faerber, P. Des Madryl, and T.M. Matelic, *Stress radiographs of the patellofemoral joint*. J Bone Joint Surg Am, 1996. **78**(2): p. 193-203.

129. Markolf, K.L., A. Graff-Radford, and H.C. Amstutz, *In vivo knee stability. A quantitative assessment using an instrumented clinical testing apparatus.* J Bone Joint Surg Am, 1978. **60**(5): p. 664-74.
130. Fithian, D.C., D.K. Mishra, P.F. Balen, M.L. Stone, and D.M. Daniel, *Instrumented measurement of patellar mobility.* Am J Sports Med, 1995. **23**(5): p. 607-15.
131. Daniel, D.M., L.L. Malcom, G. Losse, M.L. Stone, R. Sachs, and R. Burks, *Instrumented measurement of anterior laxity of the knee.* J Bone Joint Surg Am, 1985. **67**(5): p. 720-6.
132. Egusa, N., R. Mori, and Y. Uchio, *Measurement Characteristics of a Force-Displacement Curve for Chronic Patellar Instability.* Clinical Journal of Sport Medicine, 2010. **20**(6): p. 458.
133. Tanner, S.M., W.P. Garth, Jr., R. Soileau, and J.E. Lemons, *A modified test for patellar instability: the biomechanical basis.* Clin J Sport Med, 2003. **13**(6): p. 327-38.
134. Skalley, T.C., G.C. Terry, and R.A. Teitge, *The quantitative measurement of normal passive medial and lateral patellar motion limits.* Am J Sports Med, 1993. **21**(5): p. 728-32.
135. Grood, E.S. and W.J. Suntay, *A joint coordinate system for the clinical description of three-dimensional motions: application to the knee.* J Biomech Eng, 1983. **105**(2): p. 136-44.
136. Bull, A.M., M.V. Katchburian, Y.F. Shih, and A.A. Amis, *Standardisation of the description of patellofemoral motion and comparison between different techniques.* Knee Surg Sports Traumatol Arthrosc, 2002. **10**(3): p. 184-93.
137. Jolliffe, I.T., *Principal component analysis.* 2nd ed. Springer series in statistics. 2002, New York: Springer. xxix, 487 p.

## **Appendix A: Additional Table and Figures**

The femoral shape measures that were collected in the axial MR image sets for each knee specimen are displayed. The full patellar shift and tilt laxity envelopes collected with the PLI are shown for each knee. The experimental patellar shift and tilt data collected during each envelope assessment are displayed in the figures with the polynomial regression curves that were fit to the extracted data. The shift and tilt displacements under each load level through the flexion range are shown for each knee specimen. Each figure contains the laxity envelope plots for an individual knee that were calculated and then include in the PC model to assess the variation in the ten knees included in this study.

**Table A-1: Femoral shape measures quantified in the axial MR image sets for each knee specimen.**

	<b>Epicondylar Width (mm)</b>	<b>Sulcus Angle (°)</b>	<b>Lateal Trochlear Slope (°)</b>	<b>Medial Trochlear Slope (°)</b>
Knee 1	83	128	26	26
Knee 2	81	140	19	21
Knee 3	83	135	20	25
Knee 4	86	133	18	29
Knee 5	89	132	23	25
Knee 6	80	134	25	21
Knee 7	82	138	22	20
Knee 8	85	128	23	29
Knee 9	90	136	25	19
Knee 10	84	140	22	18

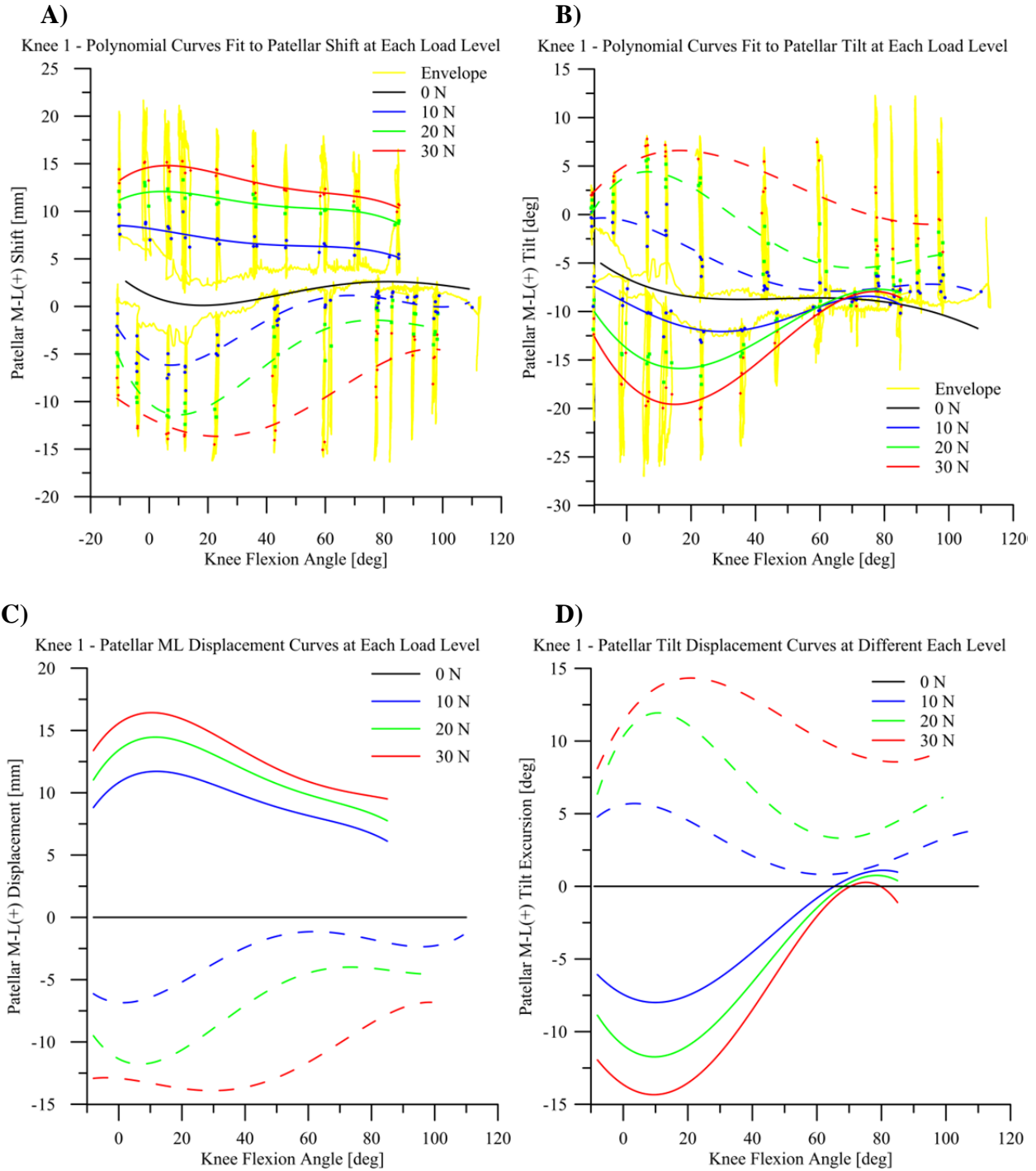


**Figure A-1: Experimental patellar shift data (A) and patellar tilt data (B) collected during PF envelope assessment for a Knee 1. Data points were extracted at each load level, and fourth-order polynomials were fit to the extracted data points (solid lines (lateral loads) and dash lines (medial loads)). Patellar shift (C) and patellar tilt (D) displacements were calculated from the polynomials at each load level through the flexion range.**

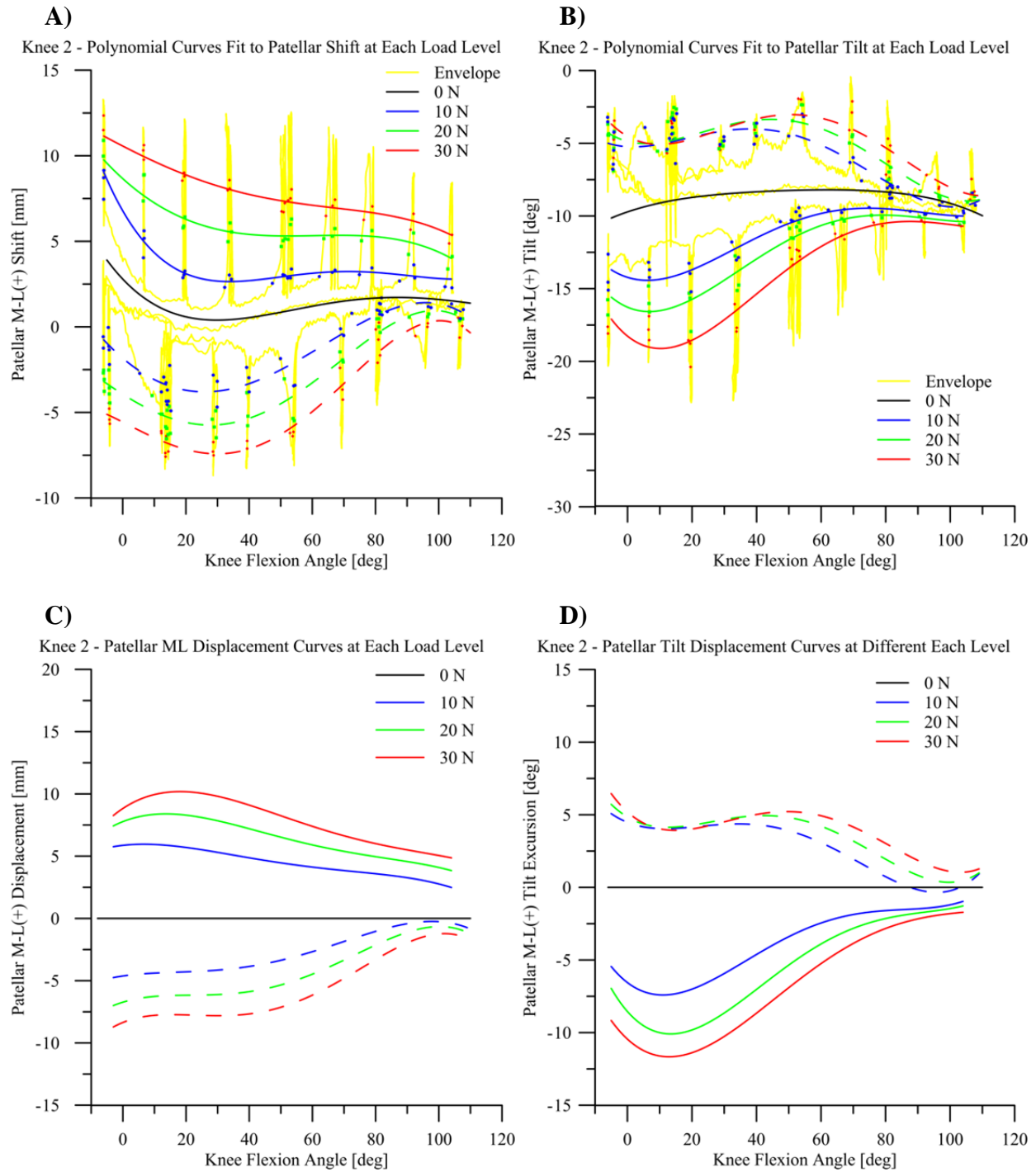


**Figure A-2: Experimental patellar shift data (A) and patellar tilt data (B) collected during PF envelope assessment for a Knee 2. Data points were extracted at each load level, and fourth-order polynomials were fit to the extracted data points (solid lines (lateral loads) and dash lines (medial loads)). Patellar shift (C) and patellar tilt (D) displacements were calculated from the polynomials at each load level through the flexion range.**

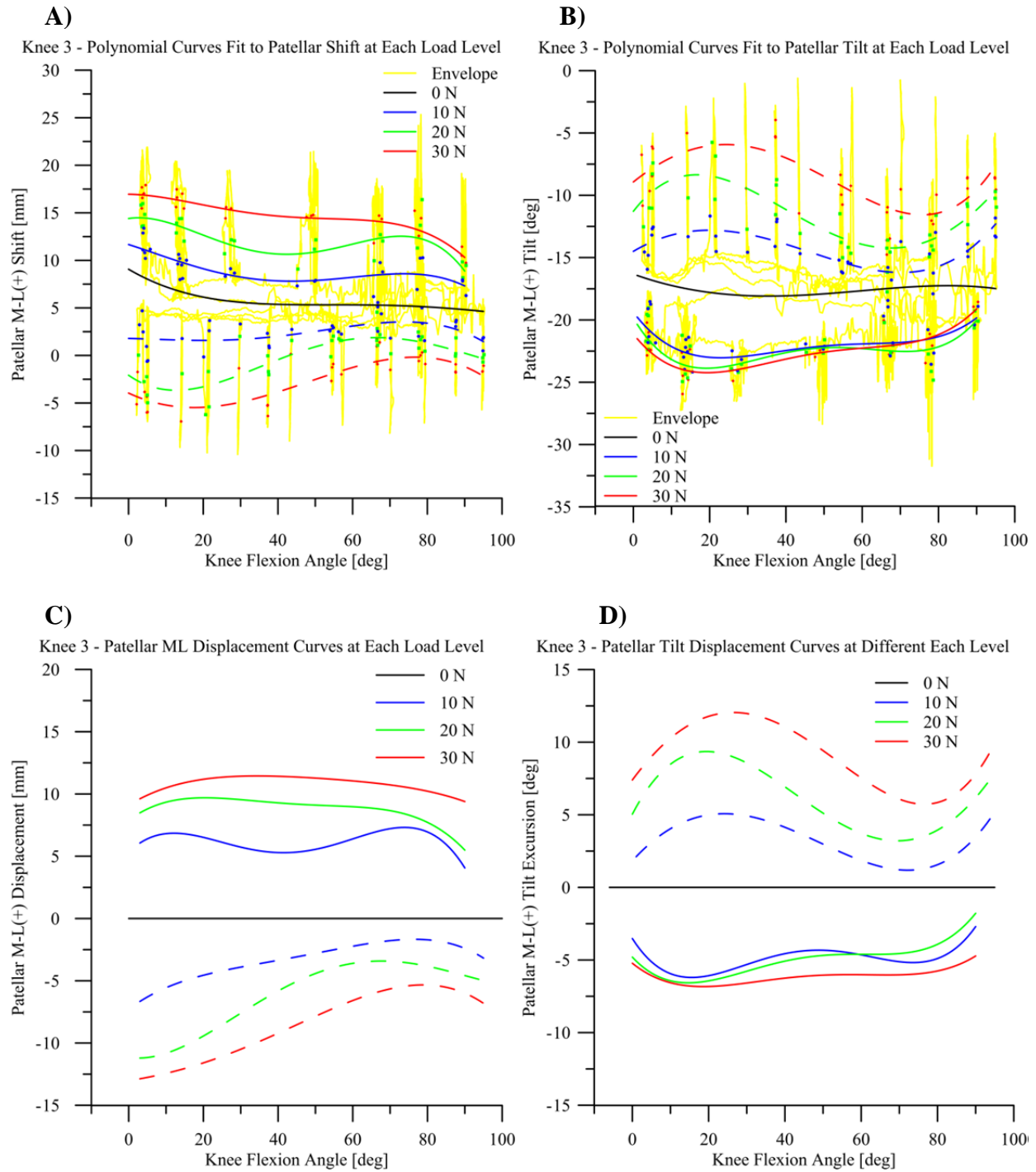


**Figure A-3: Experimental patellar shift data (A) and patellar tilt data (B) collected during PF envelope assessment for a Knee 3. Data points were extracted at each load level, and fourth-order polynomials were fit to the extracted data points (solid lines (lateral loads) and dash lines (medial loads)). Patellar shift (C) and patellar tilt (D) displacements were calculated from the polynomials at each load level through the flexion range.**

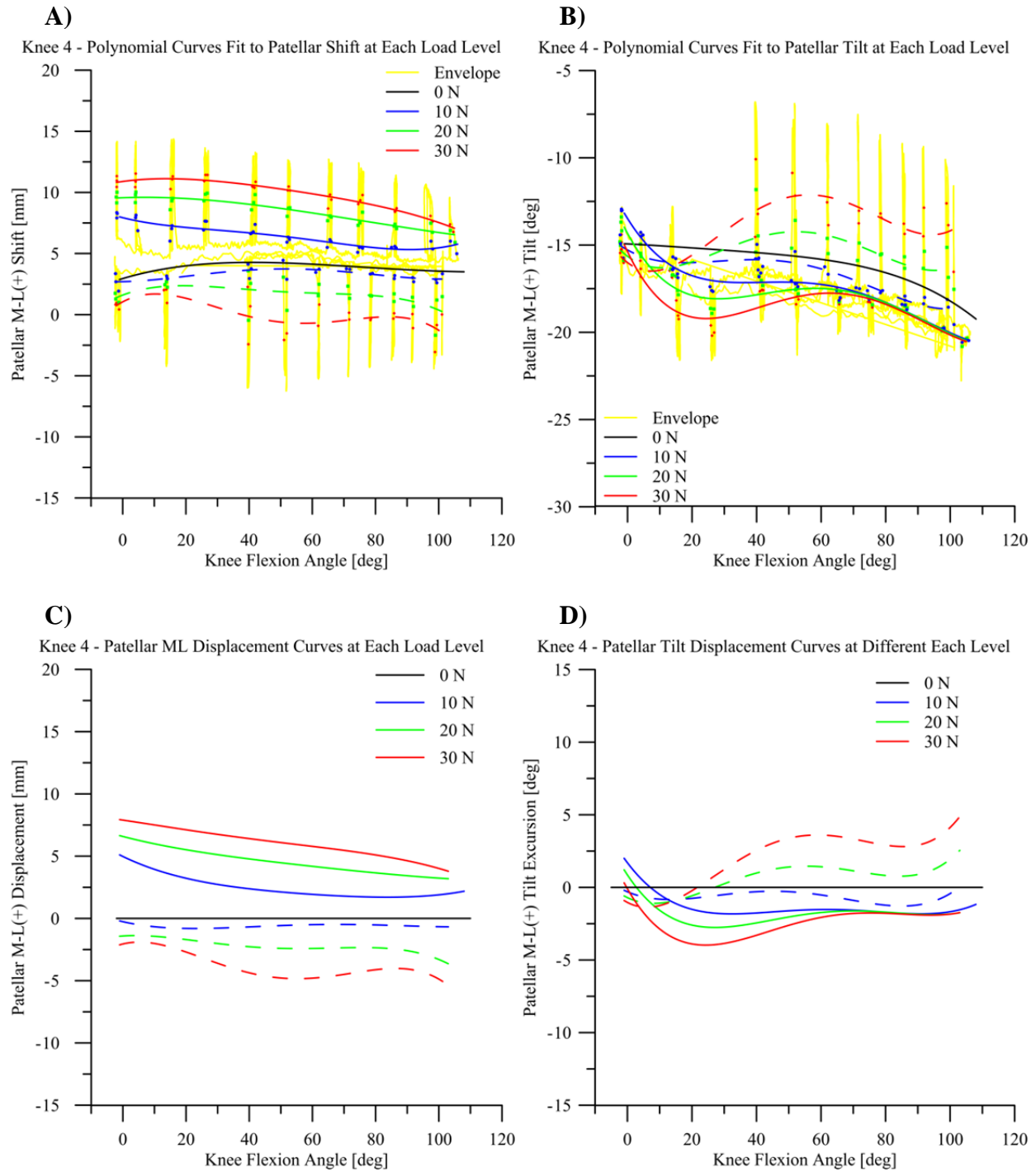


**Figure A-4: Experimental patellar shift data (A) and patellar tilt data (B) collected during PF envelope assessment for a Knee 4. Data points were extracted at each load level, and fourth-order polynomials were fit to the extracted data points (solid lines (lateral loads) and dash lines (medial loads)). Patellar shift (C) and patellar tilt (D) displacements were calculated from the polynomials at each load level through the flexion range.**

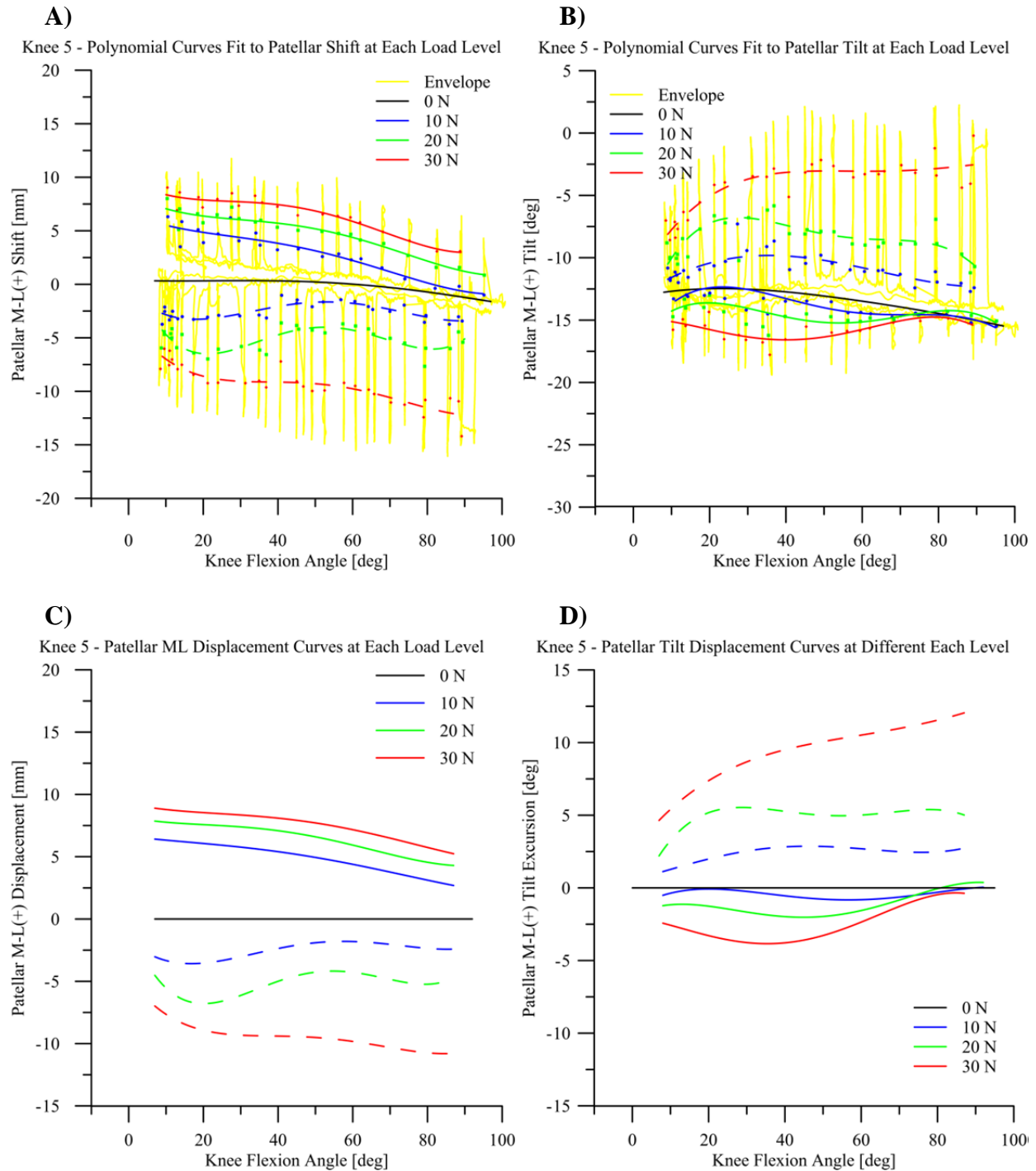


**Figure A-5: Experimental patellar shift data (A) and patellar tilt data (B) collected during PF envelope assessment for a Knee 5. Data points were extracted at each load level, and fourth-order polynomials were fit to the extracted data points (solid lines (lateral loads) and dash lines (medial loads)). Patellar shift (C) and patellar tilt (D) displacements were calculated from the polynomials at each load level through the flexion range.**

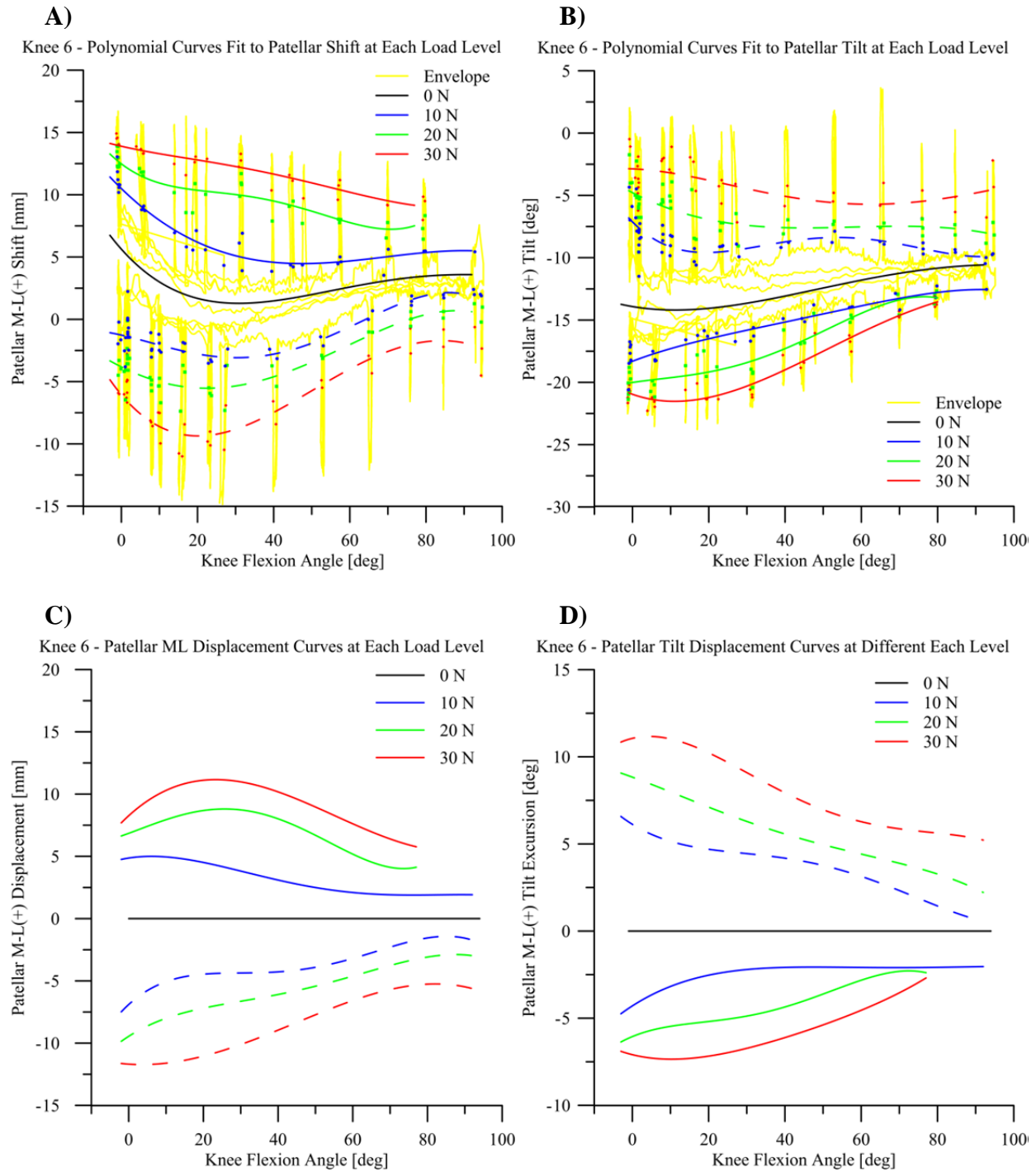


**Figure A-6: Experimental patellar shift data (A) and patellar tilt data (B) collected during PF envelope assessment for a Knee 6. Data points were extracted at each load level, and fourth-order polynomials were fit to the extracted data points (solid lines (lateral loads) and dash lines (medial loads)). Patellar shift (C) and patellar tilt (D) displacements were calculated from the polynomials at each load level through the flexion range.**

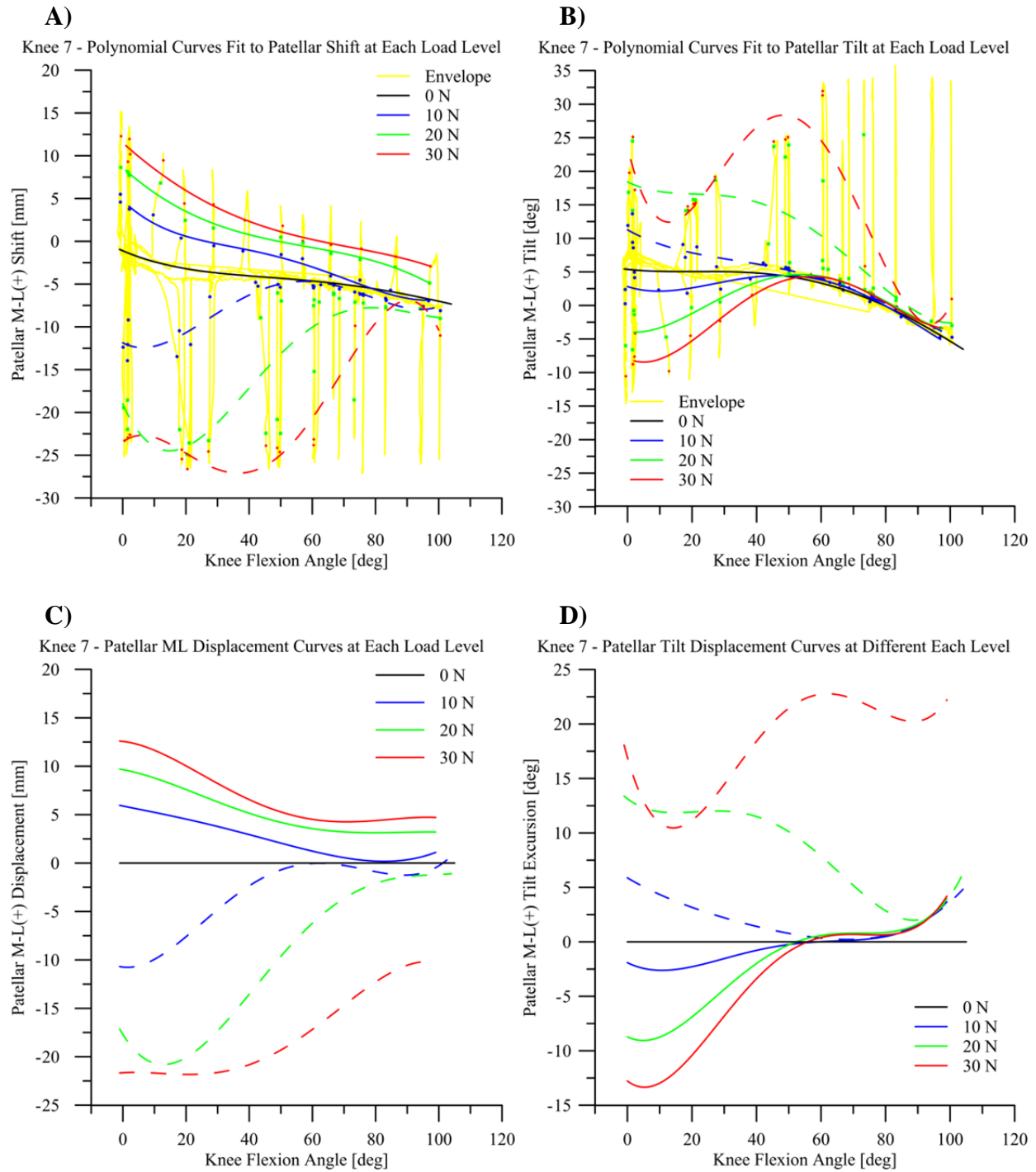


**Figure A-7: Experimental patellar shift data (A) and patellar tilt data (B) collected during PF envelope assessment for a Knee 7. Data points were extracted at each load level, and fourth-order polynomials were fit to the extracted data points (solid lines (lateral loads) and dash lines (medial loads)). Patellar shift (C) and patellar tilt (D) displacements were calculated from the polynomials at each load level through the flexion range.**

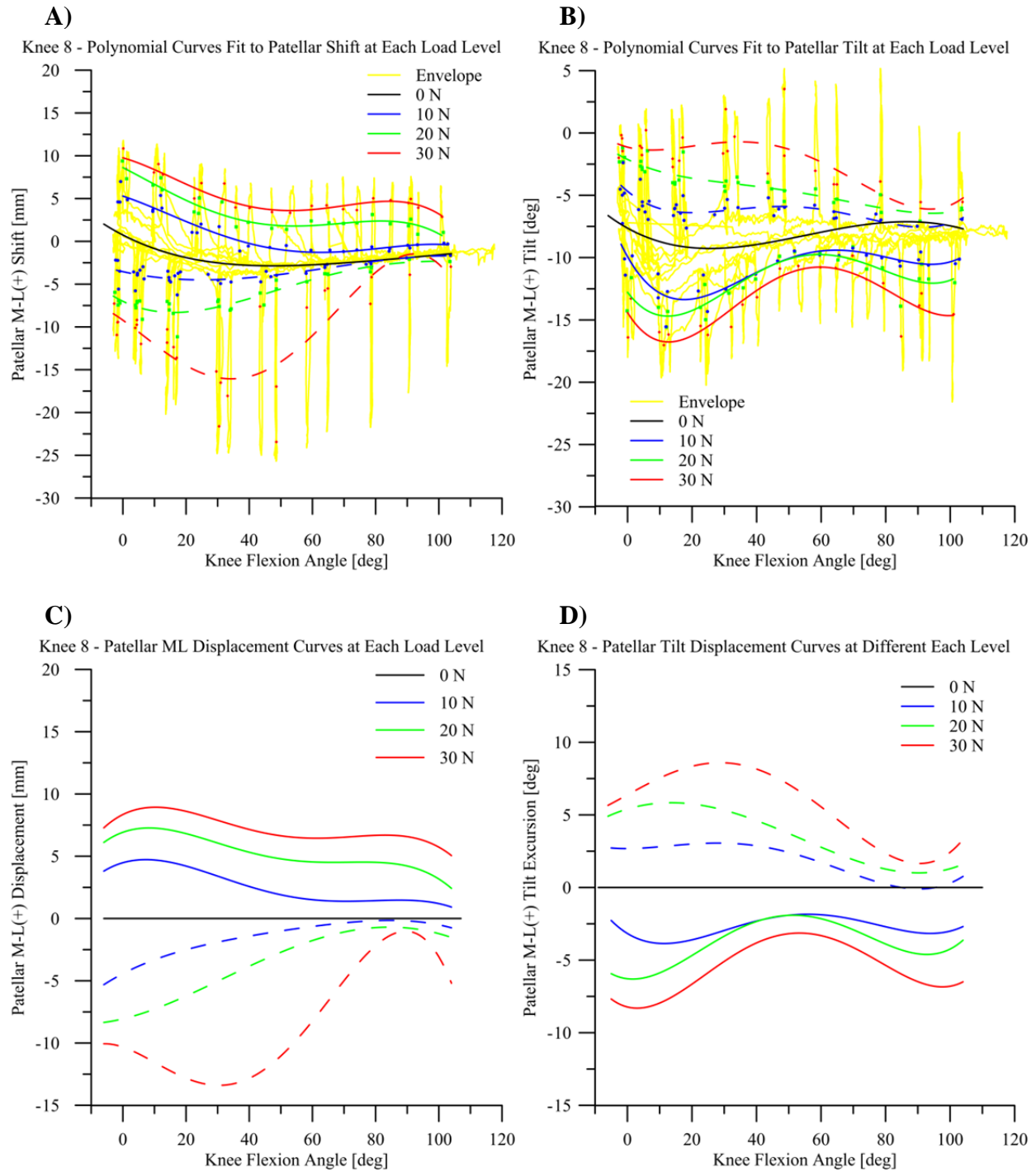


**Figure A-8: Experimental patellar shift data (A) and patellar tilt data (B) collected during PF envelope assessment for a Knee 8. Data points were extracted at each load level, and fourth-order polynomials were fit to the extracted data points (solid lines (lateral loads) and dash lines (medial loads)). Patellar shift (C) and patellar tilt (D) displacements were calculated from the polynomials at each load level through the flexion range.**

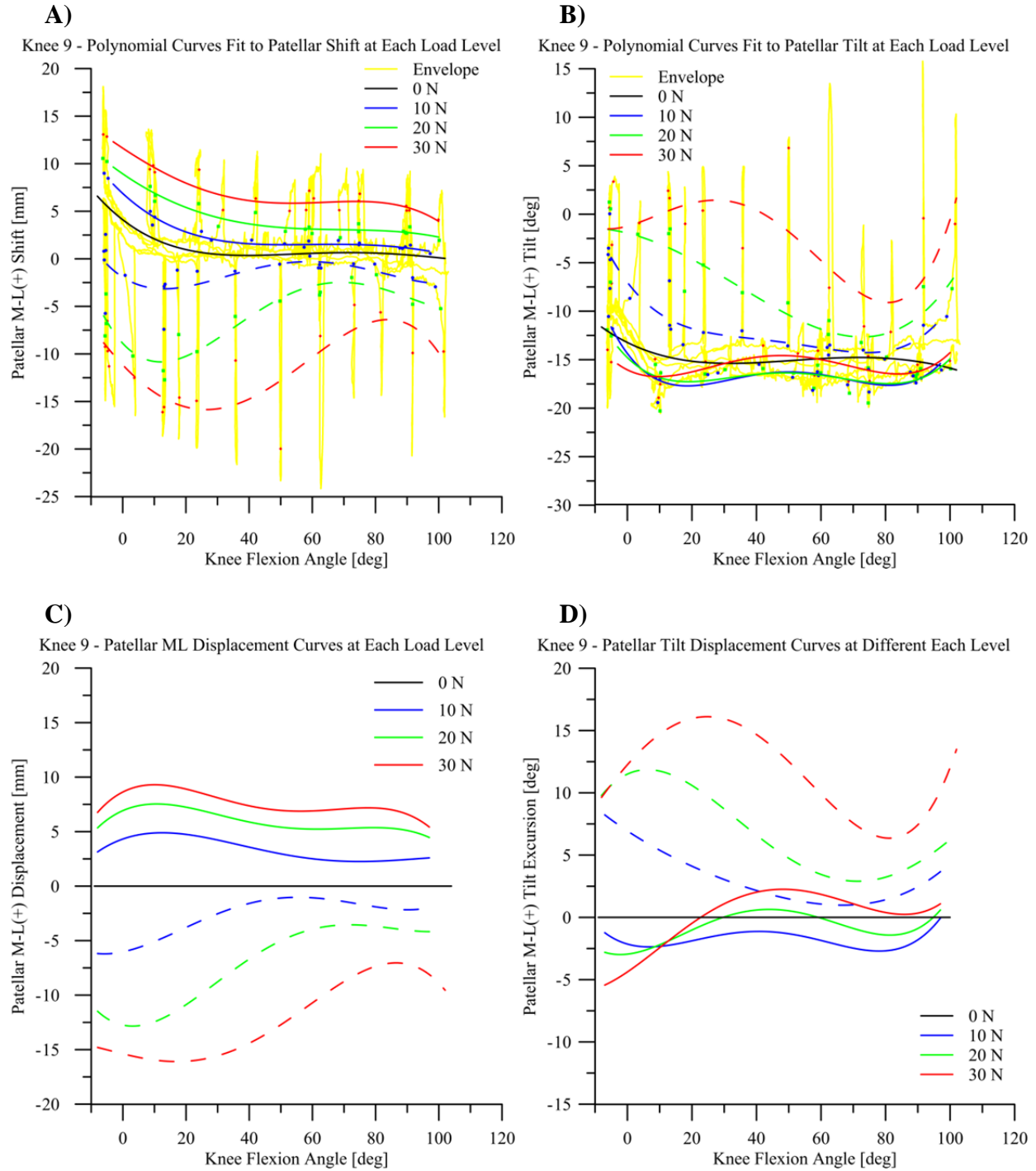


**Figure A-9: Experimental patellar shift data (A) and patellar tilt data (B) collected during PF envelope assessment for a Knee 9. Data points were extracted at each load level, and fourth-order polynomials were fit to the extracted data points (solid lines (lateral loads) and dash lines (medial loads)). Patellar shift (C) and patellar tilt (D) displacements were calculated from the polynomials at each load level through the flexion range.**

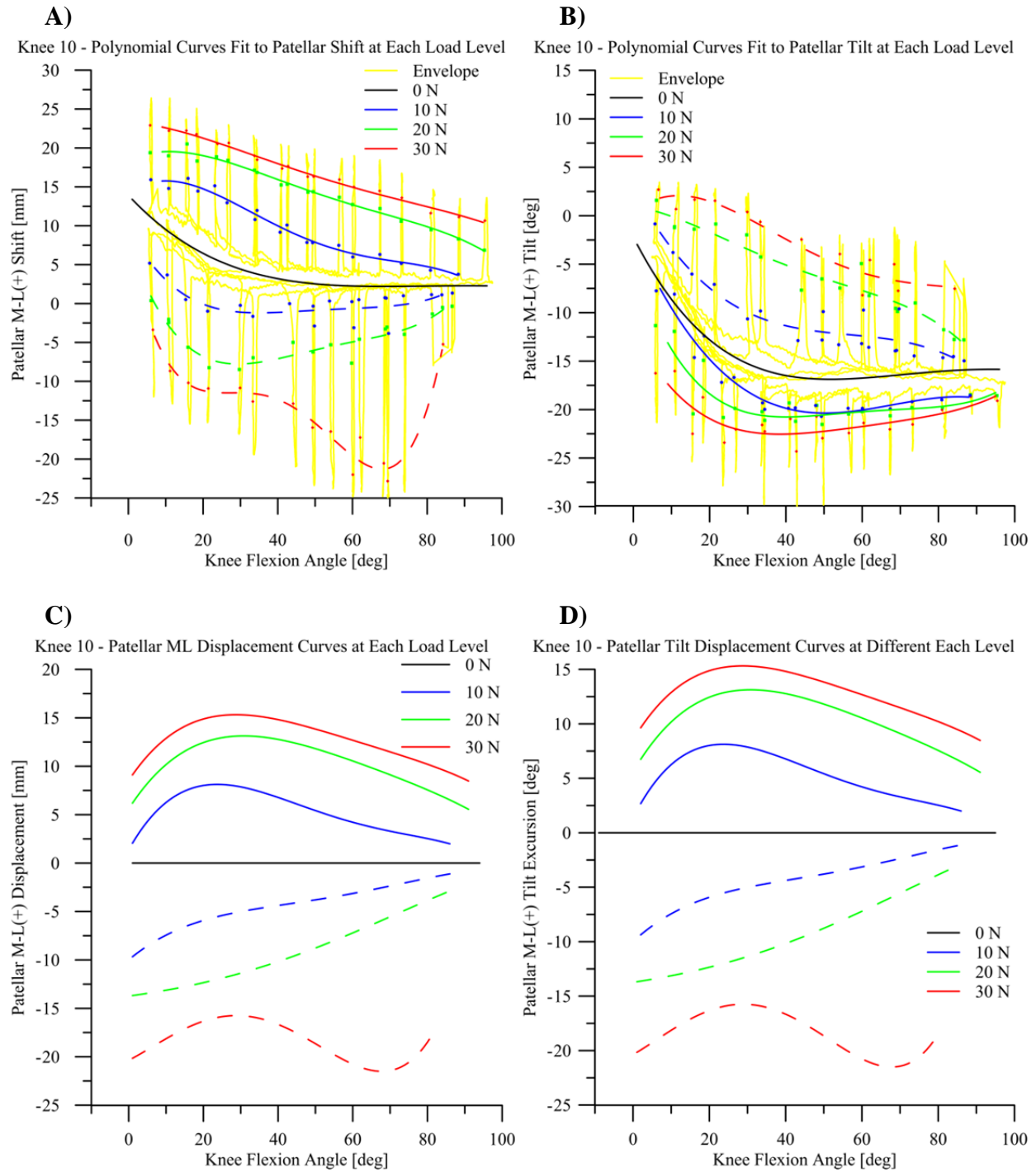


**Figure A-10: Experimental patellar shift data (A) and patellar tilt data (B) collected during PF envelope assessment for a Knee 10. Data points were extracted at each load level, and fourth-order polynomials were fit to the extracted data points (solid lines (lateral loads) and dash lines (medial loads)). Patellar shift (C) and patellar tilt (D) displacements were calculated from the polynomials at each load level through the flexion range.**